



This document is a postprint version of an article published in Marine Pollution Bulletin© Elsevier after peer review. To access the final edited and published work see <https://doi.org/10.1016/j.marpolbul.2021.113183>

Document downloaded from:



# **Assessment of marine benthic diatom communities: insights from a combined morphological–metabarcoding approach in Mediterranean shallow coastal waters.**

Javier Pérez-Burillo<sup>1,2</sup>, Greta Valoti<sup>3</sup>, Andrzej Witkowski<sup>4</sup>, Patricia Prado<sup>1</sup>, David G. Mann<sup>1,5</sup> & Rosa Trobajo<sup>1\*</sup>

<sup>1</sup>IRTA-Institute for Food and Agricultural Research and Technology, Marine and Continental Waters Programme. Ctra de Poble Nou Km 5.5, E43540, Sant Carles de la Ràpita, Tarragona, Spain

<sup>2</sup>Departament de Geografia, Universitat Rovira i Virgili, C/ Joanot Martorell 15, E43500, Vila-seca, Tarragona, Spain

<sup>3</sup>Università Politecnica delle Marche, Piazza Roma, 22, IT60131, Ancona, Italy

<sup>4</sup>Institute of Marine and Environmental Sciences, University of Szczecin, Mickiewicza 16a, 70-383 Szczecin, Poland

<sup>5</sup>Royal Botanic Garden Edinburgh, Edinburgh, EH3 5LR, Scotland, UK

\*corresponding author: [rosa.trobajo@irta.cat](mailto:rosa.trobajo@irta.cat)

1 **Abstract**

2 We investigated the advantages and disadvantages of light microscope (LM)-based identifications and DNA  
3 metabarcoding, based on a 312-bp *rbcL* marker, for examining benthic diatom communities from  
4 Mediterranean shallow coastal environments. For this, we used biofilm samples collected from different  
5 substrata in the Ebro delta bays. We show that 1) Ebro delta bays harbour high-diversity diatom communities  
6 [LM identified 249 taxa] and 2) DNA metabarcoding effectively reflects this diversity at genus-but not  
7 species level, because of the incompleteness of the DNA reference library. Nevertheless, DNA  
8 metabarcoding offers new opportunities for detecting small, delicate and rare diatom species missed by LM  
9 and diatoms that lack silica frustules. The primers used, though designed for diatoms, successfully amplified  
10 rarely reported members of other stramenopile groups. Combining LM and DNA approaches offers stronger  
11 support for ecological studies of benthic microalgal communities in shallow coastal environments than using  
12 either approach on its own.

13

14 **Key words:**

15 Diversity, environmental DNA, epibiotic, microalgae, Stramenopiles, *rbcL*.

16

## 17 1. Introduction

18 Coastal ecosystems are ecologically important because they are highly productive areas that harbour  
19 a great diversity, which is reflected in many types of ecological communities found in these  
20 systems, such as seagrass beds, sandflat communities, coral and bivalve reefs (Cloern et al., 2013).  
21 These ecosystems are also important from a socio-economic point of view as they provide  
22 numerous ecosystem services and contribute importantly to the global total (Costanza et al., 2014).  
23 Benthic diatom communities constitute an important component of these systems because of their  
24 large contribution to total production (MacIntyre et al., 1996). A recent study of seagrass beds in  
25 shallow systems (Cox et al. 2020) has shown that the contribution of diatoms can be over 80% of  
26 benthic production and that without them the seagrass beds can be net heterotrophic. In addition,  
27 they have a major role in the stabilization of sediments thanks to the production of extracellular  
28 polymeric substances (EPS) and consequently, they regulate on of nutrient fluxes and other  
29 biogeochemical processes (Cahoon et al., 1999, Sundbäck & Granéli, 1988; Sundbäck et al., 1991;  
30 Triska & Oremland, 1981; Trobajo & Sullivan, 2010). They can be found in or attached to different  
31 substrata, such as the surface of sediments (epipelon), sand grains (epipsammon), seagrasses,  
32 macroalgae, and microalgae (epiphyton), or the surface of animals including the shells of molluscs  
33 (epizoon). Each of these community types can be very species-rich (Round, 1971) and it has been  
34 shown that within communities, different species can play different roles; for instance, in tidal  
35 habitats epipellic species show differences in photophysiology and migration activity (Underwood et  
36 al., 2005). Hence, it is crucial to combine system-wide estimates of benthic diatom contributions to  
37 primary production with an understanding of the roles and functioning of the species comprising  
38 these communities. However, the morphological identifications of diatoms at the species level are  
39 difficult and require expertise in taxonomy. This is especially true for shallow coastal environments  
40 (Mann et al., 2016; Trobajo et al., 2004), despite their ecological and economic importance.

41 DNA metabarcoding has proved to be a reliable method for studying species diversity from  
42 environmental samples (Deiner et al., 2017) and has emerged as an alternative to light microscope-  
43 based identifications (LM) due to its speed, reproducibility, and cost (Kermarrec et al., 2014;  
44 Zimmermann et al., 2015). It has been broadly tested for freshwater ecological assessment based on  
45 benthic diatoms (e.g. Bailet et al., 2019; Kelly et al., 2020; Mortágua et al., 2019; Pérez-Burillo et  
46 al. 2020, Vasselon et al., 2017) and for biodiversity studies (e.g. Stoof-Leichsenring et al., 2020;  
47 Rimet et al., 2018). DNA metabarcoding has also been applied in marine environments, especially  
48 in phytoplankton studies (e.g. De Luca et al.2021; Malviya et al. 2016; Piredda et al., 2018), but  
49 rarely to the phytobenthos of coastal areas, which are very productive and species rich. Exceptions  
50 include studies of US saltmarshes (Plante et al. 2021a, b), intertidal sediments in Korea (An et al.  
51 2020), a eutrophic estuary in South Africa (Nunes et al., 2021), and sea turtle biofilms (Rivera et al.  
52 2018).

53 In the context of ongoing research into the biodiversity and functioning of Mediterranean  
54 shallow coastal habitats (e.g. Benito et al., 2015; Carballeira et al., 2017; Prado, 2018, 2020; Rovira  
55 et al. 2009), we set out to study the benthic diatom communities in these poorly known systems  
56 through the combined use of DNA metabarcoding, based on a 312-bp *rbcL* marker, and LM-based  
57 identifications. Sampling was aimed for selection of the different benthic communities dwelling on  
58 sediments, seaweeds, seagrasses and molluscs (i.e. epipelagic, epiphytic and epizoic/epilithic  
59 communities) in coastal areas of the Ebro delta. In particular, Ebro Delta bays sustain a very  
60 important shellfish aquaculture of Japanese oyster and Mediterranean mussel (Ramón et al., 2005),  
61 providing important substrata for biofilm development. Besides, the area holds one of the last  
62 remaining populations of fan mussel (*Pinna nobilis*) after major mass mortality events throughout  
63 the Mediterranean (Prado et al. 2014, 2021). Moreover, beds of the seagrasses *Cymodocea nodosa*  
64 and *Zostera noltii* are present in the area. In this paper we evaluate the advantages and  
65 disadvantages of each survey approach – morphological and molecular – and we assess whether the

66 *rbcL* marker, which was originally developed for diatom biomonitoring of freshwaters, is equally  
67 useful in marine environments, where the diversity of related groups of ochrophyte microalgae and  
68 macroalgae is much greater.

69

## 70 2. Material and Methods

### 71 2.1. Study area and sampling collection

72 Nine biofilm samples were taken in Alfacs and Fangar bays offshore from the Ebro Delta on the  
73 Mediterranean coast of the Iberian Peninsula (Fig. 1). The bays constitute semi-enclosed estuarine  
74 water bodies that receive freshwater inputs, rich in nutrients and organic matter, from rice fields that  
75 border both bays, which have led to eutrophication (Llebot et al., 2011; Prado, 2018). Alfacs Bay  
76 encompasses an area of 50km<sup>2</sup> with an average depth of ~3 m and a maximum of 6 m. Sampling in  
77 this bay was conducted by wading in a semi-sheltered area at ca. 60 cm depth near the southern shore,  
78 where the seagrass *Cymodocea nodosa* and/or the macroalga *Caulerpa prolifera* constitute the  
79 dominant benthic habitat, and where there is also an important population of *Pinna nobilis* (Prado et  
80 al., 2014, 2020, 2021). Fangar Bay is smaller, occupying 12 km<sup>2</sup>, and has an average depth of 2 m  
81 and a maximum of 4 m. Sampling in this bay was conducted within farms of the introduced Pacific  
82 oyster *Crassostrea gigas*, located in the southern area of the Bay. Physicochemical information at  
83 each sampling site is shown in Table 1.

84 Samples were collected in March 2020 and comprised seven biofilm samples and two  
85 sediment samples. Five of the biofilms were taken from the shell surfaces of *P. nobilis* (three  
86 different individuals from Alfacs Bay separated by distances in the order of 10s of metres) and from  
87 *Crassostrea gigas* (two individuals from Fangar Bay). The other two biofilm samples were taken  
88 from the surfaces of *Caulerpa prolifera* and *Cymodocea nodosa*, respectively, both from the same  
89 area of Alfacs Bay as those of *P. nobilis*. Finally, the two sediment samples were collected from the  
90 surface sediments (ca. 1-2 cm) immediately adjacent to specimens of *P. nobilis* and transported to

91 the laboratory within small containers. For collecting the biofilm samples, the surface of the  
92 organisms was scraped using a different toothbrush for each specimen. Each sample was divided  
93 into two aliquots and preserved in ethanol (to a final concentration  $\geq 70\%$ ). One was used for  
94 morphological examinations and the other for DNA metabarcoding analysis.

95

## 96 2.2 Microscopical analysis

97 Samples for morphological analysis were cleaned using concentrated (37%) hydrogen peroxide  
98 ( $\text{H}_2\text{O}_2$ ). However, prior to hydrogen peroxide samples were treated with few millilitres of 10% HCl  
99 to remove carbonates. After the reaction with carbonates ceased, samples were washed several  
100 times with deionized water. Thereafter samples were boiled with hydrogen peroxide for a few hours  
101 to oxidize the organic matter and then washed several times with deionized water at 24 h intervals.  
102 Cleaned diatomaceous suspension was dropped onto cover slips and left at room temperature  
103 overnight to dry. Permanent slides were mounted with Naphrax (Brunel Microscopes:  
104 <http://www.brunelmicroscopes.co.uk/>), which has a high refractive index. Diatom analysis was  
105 performed using a Leica DMLB microscope equipped with 100 $\times$  PlanApo objective (n.a. 1.4).  
106 Approximately 300 to 400 valves were counted in each sample. Problems in identification were  
107 resolved with scanning electron microscopy (SEM). For SEM examination, a drop of the cleaned  
108 sample was filtered onto Whatman Nuclepore polycarbonate membranes (Fisher Scientific,  
109 Schwerte, Germany). Filters were air-dried overnight, mounted onto aluminium stubs and coated  
110 with 5 nm of gold. Samples were analysed with an ultra-high field emission Hitachi SU 8020  
111 instrument at West Pomeranian University of Technology in Szczecin.

112

## 113 2.3 DNA extraction, PCR amplification and high-throughput sequencing (HTS) library preparation

114 A volume of 2 mL of each sample was centrifuged at 4 °C and 11,000 g for 20 min. Ethanol present  
115 in the supernatant was removed and the DNA contained in the remaining pellet was extracted using

116 the commercial DNA kit Macheray–Nagel NucleoSpin® Soil extraction kit (MN-Soil). A short  
117 *rbcL* region of 312 bp constituted the DNA marker and this was amplified by PCR using an  
118 equimolar mix of the modified versions of the Diat\_rbcL\_708F (forward) and R3 (reverse) primers  
119 given by Vasselon et al. (2017). In order to prepare the HTS library using a 2-step PCR strategy, a  
120 part of the P5 (TCGTCCGGCAGCGTCAG ATGTGTATAAGAGACAG) and P7  
121 (GTCTCGTGGGCTCGGAGATGTGTATA AGAGACA) Illumina adapters were included at the 5'  
122 end of the forward and reverse primers respectively. PCR1 reactions for each DNA sample were  
123 performed in triplicate using 1 µL of the extracted DNA in a final volume of 25 µL. The conditions  
124 and the reaction mix of the PCR1 were as described in Vasselon et al. (2017). All three PCR1  
125 replicates were pooled and sent to “Plateforme Génome Transcriptome” (PGTB, Bordeaux, France),  
126 where the PCR1 products were purified and used as a template for a second round of PCR (PCR2),  
127 with Illumina-tailed primers targeting the half of P5 and P7 adapters. The resulting dual-indexed  
128 amplicons were pooled for sequencing on an Illumina MiSeq platform using a V2 paired-end  
129 sequencing kit (250 bp × 2).

130

#### 131 2.4 Bioinformatic analysis

132 The sequencing facilities performed the demultiplexing of all the samples providing two fastq files  
133 per sample, one corresponding to the forward reads (R1) and one to the reverse reads (R2). Primers  
134 from all the demultiplexed MiSeq reads were removed by cutadapt (Martin, 2011) and the resulting  
135 R1 and R2 reads were processed together using the R package DADA2 (Callahan *et al.*, 2016). R1  
136 reads were truncated to 225 bases and R2 to 180 bases based on their quality profile (median quality  
137 score < 30). Reads with ambiguities or an expected error (maxEE) > 2 were discarded. The DADA2  
138 denoising algorithm was then applied to determine an error rates model to infer Amplicon sequence  
139 variants (ASVs). Chimeric ASVs were detected and discarded using the “removeBimeraDenovo”  
140 function. The taxonomic affiliations of the ASVs was determined using the database “A ready-to-



141 use database for DADA2: Diat.barcode\_rbcL\_312bp\_DADA2” (Chonova et al., 2020), which is  
142 derived from the curated diatom reference library Diat.barcode v9 (Rimet et al., 2019, available at  
143 [https://www6.inra.fr/carrtel-collection\\_eng/Barcoding-database](https://www6.inra.fr/carrtel-collection_eng/Barcoding-database) and at  
144 <https://data.inrae.fr/file.xhtml?persistentId=doi:10.15454/TOMBYZ/IEGUXB&version=10.0>); the  
145 naïve Bayesian classifier method (Wang et al., 2007) was used, with 85% set as the minimum  
146 confidence threshold. The taxonomy of unclassified ASVs was checked using the Basic Local  
147 Alignment Search Tool (BLAST) against the Nucleotide database of NCBI GenBank, with standard  
148 settings (Camacho *et al.*, 2009). Taxonomy was assigned keeping taxa with a percentage of identity  
149 higher than 97%. To allow inter-sample comparisons, all samples were resampled to the minimum  
150 number of reads recorded in any single sample (5427 reads) using the R package *phyloseq*  
151 (McMurdie & Holmes, 2013).

152

## 153 2.5 Data analyses

154 For assessing the effectiveness of the two methods in identifying taxa, the percentages of reads or  
155 cells identified to species and genus were determined. Furthermore, the percentages of species and  
156 genera recorded molecularly that were also identified by the morphological approach and vice versa  
157 were calculated. For other statistical analyses, the rarefied molecular inventory was used. To  
158 compare diatom diversity between methods and sampling sites, the Shannon–Wiener index was  
159 calculated (based on natural logarithms), using the relative abundances of taxa from the  
160 corresponding morphological and molecular inventories. The Sørensen index, based on  
161 presence/absence data, was also calculated to evaluate the similarities in diatom communities  
162 between samples. To visualize patterns in taxon composition (in LM and DNA metabarcoding  
163 inventories) among samples non-metric multidimensional scaling (NMDS) was used, based on  
164 Bray–Curtis dissimilarity matrices on ASV, species and genus relative abundance. The correlation  
165 between the distance matrices generated by both methods, using diatom species relative

166 abundances, was evaluated by computing a Mantel test (with 999 permutations). Statistically  
167 significant differences in diatom community composition at the ASV-, species- and genus level  
168 regarding the type of substratum (i.e. biofilm samples taken from *P. nobilis*, , *Crassostrea gigas*,  
169 *Caulerpa prolifera* and *Cymodocea nodosa* and samples collected from the sediment adjacent to *P.*  
170 *nobilis*) were evaluated through a permutation multivariate analysis of variance (PERMANOVA).  
171 To identify the taxa that accounted for most of the dissimilarities between the LM and DNA  
172 metabarcoding inventories, an analysis of similarity percentages (SIMPER) was performed on both  
173 species and genus relative abundance. The R package *vegan* (Oksanen et al., 2020) was used for  
174 performing all these analyses.

175

## 176 2.6. Phylogenetic analyses of non-diatom ASVs

177 Although the primers used here were designed specifically for freshwater diatom biomonitoring  
178 (Vasselon et al. 2017), they do nevertheless sometimes amplify *rbcL* from other groups of algae.  
179 For example, the ASV with most reads in the 2017 Catalan rivers dataset used by Pérez-Burillo et  
180 al. (2020, 2021) was an unknown green alga related to *Nautococcus* and *Oophila*  
181 (Chlorococcaceae), which was present in 116 of 164 samples analysed; Ochrophyta classes (sensu  
182 Adl et al. 2019) were also represented, including Xanthophyceae (e.g., *Vaucheria*) and  
183 Eustigmatophyceae (e.g., *Neomonodus*). In marine habitats the diversity of ochrophytes and red  
184 algae is much greater than in freshwaters and different green algal groups are present. Indeed,  
185 preliminary blastn analysis of our reads that were not assigned to any diatom taxon by the Bayesian  
186 classifier indicated that some ASVs belonged to different classes or phyla of algae. The majority  
187 (both in terms of ASVs and reads) were ochrophytes and we therefore performed phylogenetic  
188 analyses of the non-diatom ASVs together with GenBank sequences of selected ochrophytes to  
189 elucidate their affiliations and phylogeny. To do this, we assembled the sets of *rbcL* sequences used  
190 by Graf et al. (2020) and Wetherbee et al. (2021) and added representatives of other ochrophyte

191 classes (particularly Chrysophyceae and Synurophyceae) to provide a wide coverage of the group.  
192 We also added further Phaeophyceae that blastn analysis indicated were close to some ASVs. The  
193 sequences were aligned by eye in Mega X (Kumar et al. 2018) after initial use of Muscle (Edgar,  
194 2004), truncated to remove ragged ends and regions poorly represented among the taxa analysed,  
195 and exported for phylogenetic analysis to RAxML (Stamatakis 2014), as implemented in raxmlGUI  
196 v. 2.0 (Edler et al. 2021). A Maximum Likelihood (ML) tree was constructed with the alignment  
197 partitioned by codon position, using a GRT-Gamma model; 1000 replicates were made for the  
198 bootstrap analysis. The tree was visualized, midpoint-rooted, and prepared for publication using  
199 iTOL (<https://itol.embl.de>) (Letunic et al., 2021).

200           The affiliations of the few non-ochrophyte ASVs (Chlorophyta and Rhodophyta) were  
201 assessed by blast of NCBI GenBank.

202

### 203 2.7. Trait classification

204 Alongside analyses of diatom communities based on species composition we also classified for the  
205 different diatom taxa identified (either microscopically or molecularly) according to their ecological  
206 guilds and growth-forms. For this we largely followed Passy et al. (2007) and Rimet & Bouchez  
207 (2012) but we split the original euplanktonic group defined by Passy et al. (2007) into planktonic  
208 and tychoplanktonic groups. Thus, the resulting growth-forms were: high-profile, low-profile,  
209 motile, planktonic and tychoplanktonic. For some taxa, Passy and Rimet & Bouchez provided no  
210 information (their focus was on freshwater communities) and for these the growth-form was  
211 inferred on the basis of information in Round et al. (1990) and expert knowledge.

212

## 213 **3 Results**

### 214 3.1 Morphological inventory

215 A total of 249 diatom taxa (including varieties, forms, and species) were identified, the number per  
216 sample ranging from 40 to 75, with an average of 58.9. The most abundant diatom taxa were *Navicula*  
217 sp. 4, *Amphora helenensis*, *Amphora cf. helenensis*, *Cocconeis scutellum* var. *posidoniae*, *Navicula*  
218 *normaloides*, *Nanofrustulum shiloi*, *Cyclotella choctawhatcheeana*, *Navicula normalis*, *Cocconeis*  
219 *scutellum* and *Berkeleya fennica* (Supplementary Table 1). The 249 taxa recorded represented 73  
220 different genera and 128 different species. The number of species identified per sample ranged from  
221 25 to 47, with an average of 36.4. A total of 122 taxa (49%) could not be identified at species level  
222 but only at genus level.

223 Low profile and motile growth forms, mainly represented by species from *Amphora*,  
224 *Cocconeis*, *Navicula* and *Nitzschia*, were the predominant groups in all the samples, followed by the  
225 high-profile group (Fig. 2a), in which *Berkeleya* was the most abundant genus (Supplementary Table  
226 1). The planktonic and tycho planktonic groups were less represented and not identified in all the  
227 samples. They were more abundant in *P. nobilis* samples (Fig 2a) and were represented mainly by  
228 *Cyclotella*.

229

### 230 3.2 Molecular inventory

231 MiSeq Illumina sequencing produced a total of 176,248 raw DNA reads from the nine samples.  
232 After processing the reads through the DADA2 pipeline, 139,815 reads remained, belonging to 682  
233 ASVs, with an average of 145.1 ASV per sample (Supplementary Table 2). The maximum number  
234 of ASVs per sample was 214 (in sample E12 – *Pinna nobilis* biofilm) and the minimum 72 (in  
235 sample E15 – *Caulerpa prolifera*). 127 ASVs were classified at diatom species or genus level using  
236 the Bayesian classifier, on the basis of Diat.barcode v9 (i.e., bootstrap values at species level  $\geq$   
237 85%). The taxonomic positions of 46 further ASVs that were not allocated to species by the

238 Bayesian classifier (i.e., their bootstrap values at species level were < 85%) were resolved by blastn  
239 on GenBank and allocated to species using a percentage of identity >97% as threshold. Finally, an  
240 additional 181 ASVs that did not fulfil either of the two previous criteria were classified at genus  
241 level by using a combination of expert knowledge and examination of the most similar sequences in  
242 GenBank.

243 Altogether, the three approaches described above allowed a total of 354 of the 682 ASVs to  
244 be classified to species or genera of diatoms, with 69 species and 73 genera identified. After  
245 rarefaction was applied, these numbers were very slightly reduced (the total number of 354 diatom  
246 ASVs was reduced to 338 ASVs, accounting for 51.2% of the total of rarefied reads, comprising  
247 fully identified 69 species and 71 genera) (Supplementary Table 2). The number of species per  
248 sample ranged from 21 to 54, with an average of 37.3, and the ten most abundant diatom taxa in the  
249 inventory were: *Thalassiosira profunda*, *Achnanthes longipes*, *Berkeleya fennica*, *Nanofrustulum*  
250 *shiloi*, *Navicula* sp., *Cyclotella* sp., *Haslea howeana*, *Seminavis* cf. *robusta*, *Craspedostauros*  
251 *constricta* and *Licmophora paradoxa*.

252 Among the ASVs were several genera and species that were missed or poorly represented in  
253 the morphological dataset. One important factor was the lower detection limit of metabarcoding:  
254 even in the least productive sample (*Caulerpa* epiphytes) >5000 reads were obtained, offering the  
255 possibility to detect rare species undetectable among the c. 400 specimens per sample identified  
256 morphologically. It was noticeable too that some ASVs represented species that have very delicate  
257 or small cells. Several of these are rarely evident in any cleaned material, such as *Cylindrotheca* and  
258 some species of Cymatosirales (comprising *Arcocellulus*, *Extubocellulus*, *Papiliocellulus* and  
259 *Minutocellus* in our material). *Cylindrotheca* species are very lightly silicified and often destroyed  
260 by oxidative cleaning (Round et al. 1990). Only one sample was recorded to contain *Cylindrotheca*  
261 by LM analysis but eleven ASVs were assigned to *Cylindrotheca* by the classifier, one or more  
262 occurring in each of the nine samples.

263 Processing with DADA2 does not remove all artifactual sequences and examination of the  
264 sequences of rare diatom ASVs revealed some that could not represent functional genes since they  
265 contained one or more stop codons. The most abundant of these was ASV0569, with a total of six  
266 reads and occurring in just one of the nine samples. However, rare ASVs were not necessarily  
267 artifactual. ASV0645, with just three reads, was an exact match to GenBank accession DQ813818  
268 of *Pseudo-nitzschia delicatissima* (see also section 3.4 below).

269 Motile and planktonic growth forms predominated in most of the samples in the molecular  
270 analyses and were primarily represented by *Nitzschia* and *Navicula* (motile) and *Thalassiosira*  
271 (planktonic) (Fig. 2b and Supplementary Table 2). The exceptions were the samples taken from  
272 *Crassostrea gigas* shells, where high profile forms were dominant, and *Cymodocea nodosa* (Fig. 2b),  
273 which had approximately equal proportions of high profile and motile forms. The high-profile group  
274 was mainly represented by *Achnanthes* and *Berkeleya* species. Conversely to LM, planktonic and  
275 tychoplanktonic forms were recorded in all the samples (Fig. 2a and b), while the low-profile group  
276 was much less represented; *Nanofrustulum* and *Amphora* genera were the most important  
277 representatives for the low-profile group.

278 The most striking feature of the molecular data was the abundance in most samples (except  
279 *Crassostrea*) of *Thalassiosira profunda*, a species for which only three specimens were identified by  
280 LM (Supplementary Tables 1 and 2). Because of the systematic bias introduced by this species, we  
281 recalculated the relative abundances of the growth forms excluding *T. profunda*. The resulting graphs  
282 (Fig. 2c) showed closer agreement with the morphological data.

283

### 284 3.3 Comparative analyses of samples from different substrata

285 Taken together, the two approaches identified a total of 102 different genera, of which 43 were  
286 identified in both inventories (43.4%), and each of both methods recorded exclusively 28 different  
287 genera. At species level, both approaches identified a total of 176 different species, of which 19

288 (10.9%) were identified in both inventories; 106 and 50 were exclusively detected in the  
289 morphological and molecular inventories respectively (Supplementary Table 3).

290 The Shannon diversity index calculated on taxa relative abundances differed between  
291 inventories. For almost all the samples, the index values were higher in the LM inventory (Table 2)  
292 and the averages obtained for the LM and DNA metabarcoding inventory were 3.29 and 2.31  
293 respectively. Both approaches agreed that the highest diversity was in a sample from a shell of *P.*  
294 *nobilis* (LM = 3.74, DNA metabarcoding = 3.04; Table 2) but disagreed for the lowest diversity; in  
295 the LM inventory this was in the sample from *Cymodocea nodosa* (2.61) but in the DNA one it was  
296 in the sample from *Caulerpa prolifera* (1.59) (Table 2). A Mantel test indicated that DNA  
297 metabarcoding and LM distance matrices calculated on diatom species relative abundances were not  
298 significantly correlated (Mantel  $r = 0.31$ ;  $p$  value = 0.077).

299 The NMDS and Sørensen similarity index based on DNA metabarcoding data showed a  
300 tendency for community composition to be more similar among samples taken from the same host  
301 (Fig. 3a; Supplementary Table 4); this tendency was still evident after the *Thalassiosira profunda*  
302 ASVs were removed and the NMDS recalculated (Supplementary Fig. 1). However, these  
303 tendencies were not as obvious when NMDS and the Sørensen index were calculated using LM data  
304 (Fig. 3b; Supplementary Table 4). In particular, the two samples of *C. gigas* were widely separated  
305 from each other in the LM-based analyses but very close and separated from the rest in the DNA  
306 metabarcoding-based ones.

307 PERMANOVA confirmed the previous tendencies observed, with statistically significant  
308 differences in the community composition among different substrata for the DNA metabarcoding  
309 inventory (PERMANOVA using ASVs:  $F_{4,4} = 2.7965$ ,  $p = 0.012$ ; using species:  $F_{4,4} = 3.3896$ ,  $p =$   
310  $0.01$ ; and using genera:  $F_{4,4} = 3.5155$ ,  $p = 0.007$ ) and for the LM inventory at species level  
311 (PERMANOVA:  $F_{4,4} = 1.362$ ,  $p = 0.032$ ) but not at genus level though differences were close to  
312 being statistically significant (PERMANOVA:  $F_{4,4} = 1.6881$ ,  $p = 0.056$ ).

313 According to the SIMPER analyses, the five genera that contributed most to the discrepancy  
314 between the morphological and molecular approaches were *Thalassiosira* (18.54%), *Navicula*  
315 (10.79%), *Amphora* (9.78%), *Cocconeis* (5.80%) and *Achnanthes* (5.61%). Below the genus level,  
316 the taxon that most influenced the dissimilarity was *T. profunda*, which was identified only by DNA  
317 metabarcoding. This species appeared in all samples analysed and was responsible for 14.37% of  
318 the discrepancy between the two inventories (Table 3). The second most important taxon was  
319 *Navicula* sp.4, contributing 4.88% of the dissimilarity. It was identified only by LM, and it  
320 appeared in most of the samples (Table 3). Next was *Amphora helenensis*, which was identified by  
321 both methods, but it was much more abundant in the LM inventory. The opposite case was  
322 exemplified by *Achnanthes longipes*, a large-celled species with many chloroplasts that was much  
323 more abundant in the DNA metabarcoding inventory; it was the fourth species most influencing the  
324 dissimilarities between the two inventories (4.15%) (Table 3). A total of 83 species identified by  
325 LM lacked representative sequences in the reference library and they accounted for 16.32% of the  
326 total dissimilarities between inventories. Noteworthy among these were *Cocconeis scutellum* var.  
327 *posidoniae*, *C. scutellum*, *Navicula normaloides* and *N. normalis*, which together accounted for  
328 6.10% of the total discrepancies (Table 3).

329

#### 330 3.4 Diversity and phylogenetic analyses of non-diatom ASVs

331 Blastn and phylogenetic analyses allowed us to classify many of the non-diatom DNA reads to a  
332 class of algae and in some cases to a genus or species. In total, 41 non-diatom ASVs were analysed  
333 and allocated, a few of them with considerable hesitation, to an alga class or division. Ten of them  
334 were assigned to the Chlorophyta (and were easily recognized in the ASV alignment because all  
335 had an extra amino acid relative to the ochrophyte and red algal sequences), mostly with low  
336 similarity to any named taxon, except for *Umbraulva*, *Ulvella* and marine *Ulothrix* (the kleptoplasts  
337 of *Strombidium* sequenced for GenBank AY257112 are presumably from this genus:



338 Supplementary Table 5); one sequence was apparently related closely to an uncultured *Picochlorum*  
339 (Supplementary Table 5). The three red algal ASVs were placed more definitively, as species (or  
340 relatives) of the genera *Grania* and *Acrochaetium*, which both grow as branching filaments, and the  
341 crustose *Pneophyllum*.

342 Most of the remaining non-diatom ASVs could be assigned with varying degrees of  
343 confidence to one of 10 classes of Ochrophyta (sensu Adl et al. 2019) (Fig. 4, Supplementary Table  
344 5): Chrysophyceae (1 ASV, with low confidence), Synchronophyceae (2 ASVs), Pinguiphyceae  
345 (1 ASV), Eustigmatophyceae (1 ASV), Dictyochophyceae (2 ASVs), Pelagophyceae (7 ASVs),  
346 Raphidophyceae (2 ASVs), Xanthophyceae (1 ASV), Chrysomeridophyceae (2 ASVs) and  
347 Phaeophyceae (10 ASVs). The Phaeophyceae ASVs were mostly allied to species with simple or  
348 branched filaments, either in the Ectocarpales (*Hincksia*, *Myrionema*, *Streblonema*, *Elachista*,  
349 *Nemacystus*) or the Sphacelariales (*Sphacelaria*). Eight ochrophyte classes were unrepresented in  
350 the dataset: the predominantly freshwater Synurophyceae, the picoplanktonic Bolidophyceae, and  
351 the Olisthodiscophyceae, Aureanophyceae, Phaeothamniophyceae, Phaeosacciophyceae,  
352 Chrysoparadoxophyceae and Schizocladophyceae.

353 The only non-diatom ASV that could almost certainly be discounted as an artifact was the  
354 very rare ASV0657, which had a low similarity to *Tetraselmis* (c. 80%: Supplementary Table 5)  
355 and was represented by just three reads; this sequence contained two stop codons. However, three  
356 even rarer non-diatom ASVs, each represented by two reads (ASV0677–0679, belonging to the  
357 Rhodophyta and Synchronophyceae), were clearly not artifactual, judging by blastn assignment or  
358 phylogenetic analysis (Fig. 4, Supplementary Table 5).

359 None of the non-diatom ASVs were abundant, the only one exceeding 1% of reads in any  
360 sample being an ectocarpalean brown alga (ASV0078, related to *Nemacystus decipiens*) in one of  
361 the *Pinna* biofilms (E12 – *Pinna nobilis* biofilm). The most widespread was ASV0183, an  
362 unclassified eustigmatophyte that was found in all five *Pinna* biofilm and sediment samples but

363 nowhere else (Supplementary Table 5). Another possibly significant association was between the  
364 brown alga *Streblonema maculans* and *Crassostrea. Pinna* biofilms were a rich source of non-  
365 diatom ASVs, especially in sample E12 (*Pinna nobilis* biofilm).

366

#### 367 4. Discussion

##### 368 4.1. Diatom diversity in shallow coastal environments is very high and DNA metabarcoding is a 369 promising tool for studying it.

370 Our results demonstrate that the shallow coastal ecosystems studied here harbour a very rich diatom  
371 community. A total of 126 species were identified by morphology (LM); this is remarkably high  
372 when compared with previous studies on coastal environments based on a much larger sampling  
373 effort (e.g., 68-328 diatom taxa from 21-165 samples; Lobban et al., 2012; Facca & Sfriso, 2007;  
374 Kanjer et al., 2019; Virta et al., 2019). To these 126 species identified by LM, an extra 50 were  
375 added by metabarcoding. Furthermore, the large number of taxa identified only at generic level or  
376 above in both LM and DNA metabarcoding, may indicate that the total number of diatom species in  
377 the study area is very much higher. Comparisons with freshwater benthic communities are also  
378 instructive. The average diversities of our nine samples exceeded those of periphyton samples from  
379 Catalan rivers (for which we had many more samples, Supplementary Table 6), whether the  
380 approach taken was metabarcoding or microscopical analysis, emphasizing how rich the diatom  
381 communities of the marine benthos can be.

382 Hence, this first survey of some of the substrata in the Ebro Bays suggests the area is a hot-  
383 spot of diatom biodiversity and provides a first step towards understanding how this biodiversity  
384 originates and is maintained and the ecological roles that it performs. For instance, diatom biofilms  
385 in shallow coastal ecosystems are known to play a major role in sediment stabilization and in  
386 providing habitat and food for other organisms (references in Trobajo & Sullivan, 2010; see also  
387 Camps-Castellà et al.2020 for a relevant example from Ebro Bays); moreover, a recent study of

388 benthic diatoms in the Baltic Sea has shown that high diatom diversity supports high ecosystem  
389 productivity (Virta et al., 2019). Our study demonstrates that DNA metabarcoding based on the  
390 short 312-bp *rbcL* marker also constitutes an efficient method for surveying diatom biodiversity in  
391 coastal ecosystems. The effectiveness of the method was reflected in that 1) it recorded the same  
392 number of genera as the LM method did, 2) a high proportion of the genera (43.4%) identified by  
393 LM were also recorded by DNA metabarcoding and 3) a high number of genera (43) were  
394 exclusively identified by DNA metabarcoding. Nevertheless, the LM method showed a greater  
395 efficiency for identifying taxa at species level, which was mainly caused by the lack of  
396 representative sequences in the DNA reference library for many common species, which  
397 consequently could not be retrieved when the molecular approach was applied (further discussion in  
398 section 4.3). Despite this limitation, similarity analyses calculated on the DNA metabarcoding  
399 inventory (at ASV, species and genus level) revealed a highly-structured molecular signal,  
400 suggesting therefore that our *rbcL*-based metabarcoding was able to discriminate different shallow  
401 coastal habitats, as in some other recent studies using other DNA markers (e.g. Bombin et al., 2021;  
402 Jeunen et al. 2018; Plante et al., 2021a). In addition, the habitat preferences hinted at by DNA  
403 metabarcoding could also indicate a degree of host-specificity among diatom taxa. However, our  
404 study was not designed to investigate these aspects in detail but to explore the feasibility of using  
405 *rbcL* metabarcoding to study the benthic diatom communities of shallow coastal habitats. Therefore,  
406 another study with a greater sampling effort and strategy (e.g., to have matching samples from the  
407 two Ebro bays for those hosts present in both; more replication etc) will be needed before any  
408 further conclusions can be drawn.

409         Regarding diatom composition, it was noticeable that a higher proportion of the taxa  
410 identified by LM corresponded to the low profile and motile groups, the genera *Amphora*, *Navicula*,  
411 *Cocconeis*, *Nitzschia* and *Halamphora* being particularly abundant. These have been recorded as  
412 important members of epiphyte communities in the Mediterranean (Car et al., 2019, Mabrouk et al.,

413 2014) or as epizoic on the shells of *P. nobilis*, *C. gigas* and other molluscs (e.g., Andriana et al.,  
414 2021; Barillé et al., 2017; D’Alelio et al., 2011; Totti et al., 2011). Conversely to LM, DNA  
415 metabarcoding better represented the planktonic group. Some planktonic taxa that were only  
416 recorded in our benthic samples by DNA metabarcoding have been previously reported as ‘epizoic’  
417 or ‘epiphytic’ in other studies. Examples are *Actinoptychus octonarius*, which has been reported  
418 elsewhere as occurring on *Pinna nobilis* (Politis 1949, cited by Round, 1971), and *Asterionellopsis*,  
419 found on the seagrass *Posidonia oceanica* (Mabrouk et al., 2014). However, although it is possible  
420 that these two are genuinely benthic or tychoplanktonic, it is also possible that the cells represent  
421 sedimented phytoplankton: the much lower limit of detection of the metabarcoding approach makes  
422 it much easier to detect occasional cells or colonies displaced from their normal habitat. Another  
423 planktonic species, *Thalassiosira profunda*, is considered in detail below.

424

## 425 4.2 Opportunities of DNA Metabarcoding

### 426 4.2.1 Detection and discrimination of tiny or delicate species

427 One advantage of the metabarcoding approach is that it is more likely to pick up small and/or  
428 delicate species. We recorded *Cylindrotheca* and Cymatosirales species in the metabarcoding  
429 dataset, but almost none in the morphological inventory. The *Cylindrotheca closterium* complex is  
430 commonly reported from coastal marine phytoplankton samples and it is probably mostly  
431 tychoplanktonic. However, these samples are often counted without prior cleaning, whereas benthic  
432 samples are not generally examined before oxidative cleaning because of the difficulty of observing  
433 sufficient frustule detail in intact biofilms or sediment samples. Hence many records of  
434 *Cylindrotheca* have probably been lost. One of the Cymatosirales that we recorded with  
435 metabarcoding, *Papiliocellulus simplex*, was first described from intertidal sand at two localities in  
436 Great Britain (Gardner & Crawford, 1992) and has subsequently been recorded only planktonically  
437 from the Liguro-Provencal basin of the Mediterranean (where it was ‘extremely rare’ at two

438 stations: Percopo et al., 2011) and from several localities around Australia, mostly from  
439 metagenomic data [GBIF query 19 July 2021]. A final example of a small species easily missed or  
440 misidentified in light microscopy is *Gedaniella panicellus*, which was detected by DNA at  
441 frequencies of 0.1–1% in all but one sample but was not recorded at all in LM. This species was  
442 recently described by Li et al. (2018), who noted the difficulties of unambiguous identification by  
443 LM. Our ASV differed from the reference sequence (MF092953) by 1 bp and our record extends  
444 the known range to Europe from S. Africa and China, and from muddy rockpools to epizoic and  
445 epiphytic diatom communities.

446

#### 447 4.2.2 Rare species

448 Another benefit of metabarcoding is the possibility of detecting species that are too rare to be found  
449 in routine LM cell counts. It is usually unrealistic to count more than a few 100s of valves per  
450 sample in LM, but it is common to obtain 1000s or 10000s of reads with metabarcoding. However,  
451 rare ASVs need to be treated with some caution, because amplification and sequencing can generate  
452 errors. Indeed, a few of our ASVs seem to be artifacts, despite the error modelling and correction  
453 incorporated in DADA2, since they contained stop codons. It is much more difficult to detect errors  
454 (e.g., in the third codon position) that do not affect the amino acid coded for. Errors can be  
455 minimized by imposing an arbitrary criterion – like a minimum number of reads – to try to avoid  
456 including artifactual sequences. However, our data illustrate (e.g., the rare ASVs identified as  
457 *Pseudo-nitzschia delicatissima*, *Acrochaetium*, *Pneophyllum* and *Synchroma*: see sections 3.2, 3.4)  
458 what would be lost by imposing such a limit. The rarest ASVs can be genuine.

459

#### 460 4.2.3 Primers designed for diatoms successfully amplify some non-diatom species.

461 The primers we used were originally designed for use in freshwaters, for biomonitoring and  
462 biodiversity studies of diatoms (Vasselon et al. 2017). Our study is one of the first to apply the same  
463 primers in marine environments and reveals that the ‘diatom-specific’ primers do in fact amplify a  
464 wide variety of other marine microalgae, and even some green and red algae. The phylogenetic  
465 analyses revealed ASVs belonging to nine different non-diatom classes in the Ochrophyta. Some of  
466 these, not surprisingly, were brown algae (various Ectocarpales and Sphacelariales), which probably  
467 formed part of the macroscopic structure of the attached communities (though perhaps surprisingly,  
468 some also occurred in the sediment samples), but others were microalgae, including some that are  
469 seldom recorded. Rather than a weakness of the HTS protocols, as suggested by Grant et al. (2021),  
470 we would argue that this ‘contamination’ of the diatom data is not only tolerable (since the  
471 proportion of non-diatom reads was low – c. 1% of the total; for comparison, 25% of the Ion  
472 Torrent 18S rDNA reads obtained by Plante et al., 2021b, were non-diatoms) but a valuable bonus,  
473 especially because many of the microalgae recorded are probably small and morphologically simple  
474 (judging by the nearest relatives that can be identified in GenBank) and will therefore be easily  
475 overlooked using microscopy or culturing. Especially interesting was the discovery of ASVs related  
476 to the amoeboid alga *Synchroma pusillum* (recently described by Schmidt et al., 2012) and the  
477 coccoid *Pinguicoccus pyrenoidosus* (which is difficult to identify in LM due to its small cell  
478 diameter of 3-8  $\mu\text{m}$ : Andersen et al., 2002), and lineages of Pelagophyceae and  
479 Chrysomeridophyceae. The phylogenetic analyses also revealed one ASV closely related to the  
480 raphidophyte species *Chattonella subsalsa*. This species has been reported, among other species of  
481 *Chattonella*, to produce red tides and fish kills (Lewitus et al., 2008); the reads came from one of  
482 the sediment samples but could perhaps represent stray cells from the bay phytoplankton. Thus,  
483 these analyses illustrate the potential of DNA metabarcoding, even when based on primers designed

484 for diatoms, for identifying at least some of the other microeukaryote taxa also present in the  
485 community, including ecologically or economically relevant taxa.

486

#### 487 4.3 Discrepancies between the LM and metabarcoding results

##### 488 4.3.1 The case of *Thalassiosira profunda*.

489 The greatest dissimilarities between the results obtained by the two methods, morphological and  
490 metabarcoding, were attributable to one particularly small, delicate species, the centric  
491 *Thalassiosira profunda*. This was by far the most abundant species recorded by DNA  
492 metabarcoding but only three specimens were identified by LM (2 and 1 respectively in the *C.*  
493 *prolifera* and *C. nodosa* samples). These were found after an additional exhaustive examination of  
494 the samples was performed, beyond the normal 300–400 count and prompted by the metabarcoding  
495 data, to be sure that this species had not been overlooked in LM. *Thalassiosira profunda* is an  
496 extremely small species (valve diameter 1.25–5.5 µm), generally regarded as planktonic, which is  
497 very widely distributed (Percopo et al., 2011, Li et al., 2013, Park et al., 2016, Guiry 2021). The  
498 almost complete absence of this species from the morphological counts, which can alternatively be  
499 described as gross overrepresentation in the metabarcoding dataset, requires special explanation,  
500 because such overrepresentation is generally associated with large-celled species, such as *Ulnaria*  
501 *ulna*, *Pinnularia viridiformis* or *Navicula lanceolata* (Vasselon et al., 2018, Kelly et al., 2020),  
502 because they have a larger number of copies of *rbcL* per cell.

503 Several hypotheses might explain why *T. profunda* was abundant in the DNA reads but  
504 extremely rare from the LM inventory. None of them can be discounted entirely; all of them have  
505 consequences for planning and interpreting morphological and metabarcoding studies of marine  
506 benthic diatoms.

- 507 1. *T. profunda* could be detected almost exclusively by metabarcoding because diatoms with  
508 tiny valves are easily overlooked and difficult to identify in LM (e.g., see Belcher &  
509 Swale, 1986). In the present case, such an explanation can be discounted, given the  
510 abundance implied by the molecular data (especially taking into account the likely low  
511 *rbcL* copy number per cell) and given that all slides were examined in detail using a  $\times 100$   
512 objective. Furthermore, our re-examination of the slide preparations after analysing the  
513 metabarcoding data confirmed the almost complete absence of *T. profunda*, while no other  
514 *Thalassiosira* species were recorded as abundant in LM. However, the greater number of  
515 very small-celled and delicate diatoms (e.g. of Thalassiosirales or Cymatosirales) in many  
516 marine habitats, relative to freshwaters, means that there is greater potential for  
517 discrepancies between molecular and morphological datasets in marine studies.
- 518 2. Valves of delicate species like *T. profunda* can be destroyed during preparation for LM, as  
519 has been reported for the weakly-silicified cells of the freshwater *Fistulifera saprophila*  
520 (Kelly et al., 2020; Pérez-Burillo et al., 2020; Zgrundo et al., 2013). Small size also  
521 predisposes them to be lost, since centrifugation and sedimentation during washing steps  
522 will be less effective (e.g., Andrews, 1972). The solution is clearly to examine material  
523 before it is cleaned or retain aliquots for examination later. Unfortunately, we did not do  
524 this, but the detection of a few intact valves of *T. profunda* in the *Caulerpa prolifera* and  
525 *Cymodocea nodosa* samples, following an exhaustive search for the species, undermines  
526 destruction as a reason for ‘overrepresentation’ in the molecular dataset.
- 527 3. The molecular signal captured for *T. profunda* may not be contemporary with the  
528 morphologically characterized benthic communities but come from an earlier bloom.  
529 Some planktonic species form resting stages following a bloom (McQuoid & Hobson  
530 1996; Inoue & Taniguchi, 1999; Sugie & Kuma, 2008), leading to the deposition of a  
531 large numbers of resting spores in the sediment. These might be detectable using DNA but  
532 more difficult by LM due to morphological differences from the vegetative cells (cf.



533 Kuwata & Takahashi, 1999). However, this strategy is not known to occur in *T. profunda*.  
534 In any case, diatom resting spores and resting cells are usually more robust than vegetative  
535 cells (Krawczyk et al., 2012) and should have been found in our material if present.  
536 Alternatively, an earlier bloom of *T. profunda* could perhaps have left a molecular trace  
537 even though the frustules had redissolved *in situ*. A moderate abundance of DNA reads of  
538 *Thalassiosira* and other planktonic species, including *T. profunda*, was recently reported  
539 in saltmarsh sediments in S Carolina, USA, by Plante et al. (2021a), who suggested this  
540 could reflect deposition of faecal pellets or recent phytoplankton blooms. However, their  
541 study did not include accompanying cell counts from LM.

542 4. Finally, it is possible that intact *T. profunda* cells were present in the samples but lacked  
543 frustules, so that they were undetectable in material prepared for microscopy. As far as we  
544 know there is no confirmed report of *free-living* diatoms lacking a silica cell wall, apart  
545 from some morphotypes of *Phaeodactylum* (Round et al. 1990), but this does not mean  
546 that none exist. But wall-less diatoms certainly do occur as endosymbionts, for example in  
547 some foraminifera (Lee 2011) and dinoflagellates (Yamada et al., 2020), while other  
548 foraminifera and dinoflagellates ingest diatoms and jettison the frustules, retaining their  
549 chloroplasts (as ‘kleptoplasts’) for days or months afterwards (e.g., Pillet et al., 2011,  
550 Yamada et al., 2019), and hence also, perhaps, their *rbcL*. In freshwaters, some  
551 *Thalassiosirales* are known to be endosymbionts of dinoflagellates (e.g., Takano et al.,  
552 2007; You et al., 2015), while in marine environments chloroplasts of *Thalassiosirales* are  
553 retained by some foraminifera, e.g., *Elphidium* (Pillet et al., 2011) and *Nonionellina*  
554 species (Jauffrais et al., 2019), at least one of which (*Elphidium*) occurs in the Ebro Bays  
555 (Benito et al., 2016).

556 The possibility that *T. profunda* could have been living endosymbiotically or as  
557 kleptoplasts in the communities we sampled receives further specific support from the  
558 study of Schmidt et al. (2018), who looked at the endosymbionts of the benthic

559 foraminifera *Pararotalia calcarioformata* growing in the East Mediterranean. Among the  
560 endosymbiotic diatoms they extracted and cultured from *P. calcarioformata* was one  
561 species identified and illustrated as *Minidiscus* sp. (Schmidt et al., 2018), which we would  
562 identify instead, from the specimen illustrated (op. cit., fig. 4.12), as *T. profunda*. In any  
563 case, it is clear that several Thalassiosirales do occur without frustules in marine  
564 environments, providing a possible reconciliation of our molecular and morphological  
565 data. The potential of kleptoplasts to confuse metabarcoding results extends beyond the  
566 photic zone, since functioning diatom kleptoplasts (again from Thalassiosirales, though  
567 apparently of *Skeletonema* not *Thalassiosira*) have been recorded, with intact *rbcL*, from  
568 depths of more than 500 m in the foraminifer *Nonionella stella* (Gomaa et al., 2021).

569

#### 570 4.3.2 The effects of taxonomic resolution, reference library and gene copy number

571 Another important reason for the discrepancies observed between methods was the impossibility of  
572 identifying some taxa at species level. Marine littoral diatoms have been much less studied than  
573 their freshwater counterparts in rivers and lakes, so that several species in our samples – some of  
574 them abundant – remained unidentified at species level in LM, despite the great taxonomic effort  
575 and resources applied (including thorough LM identifications supported by SEM and TEM). The  
576 number of taxa identified as sp. or confer (cf) or affinis (aff) illustrates the incompleteness of the  
577 taxonomy underlying the morphological approach. This was particularly true for *Amphora* and also  
578 for *Navicula*, since a total of eight *Navicula* species could not be identified to known species. One  
579 of these, *Navicula* sp. 4 was very abundant and contributed greatly to the discrepancies between the  
580 LM and metabarcoding outputs. The prevalence of *Navicula* spp. without a species assignment in  
581 epibiotic communities has been shown also in other recent studies (e.g., Andriana et al., 2021; Car  
582 et al., 2019; Kanjer et al., 2019; Medlin & Juggins, 2018).

583           Concerning the metabarcoding inventories, the impossibility of reaching species-level  
584 identifications of the ASVs was often due to the incompleteness of the reference library since many  
585 species identified by LM lack representative DNA sequences, again mainly due to understudied  
586 environments. Diat.barcode (Rimet et al., 2019) aims to list and check all available *rbcL* sequences  
587 for diatoms, whether marine, coastal, or freshwater, but it depends to a considerable extent on what  
588 sequences have been deposited in NCBI GenBank, which reflects historical trends in systematic and  
589 other research. Overall, the data available show a strong bias towards freshwater diatoms, which  
590 account for around 60% of the *rbcL* entries in Diat.barcode v. 9 (>4500 sequences), despite the  
591 greater diversity of marine diatoms. Perhaps not surprisingly, therefore, many of our ASVs were not  
592 assigned to a species, or even a genus, by the Bayesian classifier. The contrast with freshwater  
593 biomonitoring analyses is illustrated in Supplementary Table 7 which shows (for the marine  
594 samples and two campaigns of metabarcoding in Catalan rivers) the proportions of the ASVs that  
595 find exact matches with reference sequences or matches at 95–99% similarity levels: the marine  
596 analysis lags well behind.

597           The incompleteness of the reference database explained c. 16% of dissimilarities between  
598 methods and some of the species missed are known for being important components in the epizoic  
599 and epiphytic diatom communities, so they could be considered priorities for future barcoding.  
600 Among them are several *Navicula* species, including *N. normaloides*, *N. normalis* and *N. subagnita*;  
601 these taxa were identified in all or most of the samples, indicating their importance in the study  
602 area. *N. normaloides* and *N. subagnita* have also been recorded as epiphytic on leaves from  
603 *Posidonia oceanica* and *Caulerpa taxifolia* in the Adriatic Sea (Kanjner et al., 2019; Car et al.,  
604 2019). It is important to emphasize, however, that in many cases the lack of representative  
605 sequences only partially prevents interpretation of metabarcoding data, though it reduces the  
606 resolution achieved. For example, despite the lack of representative sequences for the particular  
607 *Navicula* species known (from LM) to occur in our samples, the coverage of the genus in the

608 reference dataset was sufficient for the classifier to assign many ASVs at genus level. These  
609 assignments could then be checked by individual blastn searches and can be examined further in  
610 future by phylogenetic approaches, as with the non-diatom ASVs.

611 Other important species underestimated by DNA metabarcoding due to lack of reference  
612 sequences were *Cocconeis* species, notably *C. scutellum* and *C. scutellum* var. *posidoniae*. Both are  
613 cosmopolitan taxa and important components of the attached diatom communities (e.g., De Stefano  
614 et al., 2008, Polifrone et al., 2020; Ryabushko & Ryabushko, 2000; Witak et al., 2020). Overall, the  
615 genus *Cocconeis* was very poorly represented by DNA metabarcoding despite the very high  
616 diversity of *Cocconeis* species revealed by LM. Furthermore, and contrary to what we found with  
617 *Navicula* species, only a small proportion of reads and ASVs unclassified at the species level by the  
618 Bayesian classifier could be convincingly related to *Cocconeis* even at genus level. This can be  
619 explained by the fact that the reference database contains few *Cocconeis* (and almost all of them are  
620 freshwater species whose relationship to the marine species remains unknown), making it  
621 impossible for the classifier to assign ASVs to *Cocconeis* or related genera at any level. A few  
622 ASVs were tentatively identified as possible *Cocconeis* or Cocconeidaceae species on the basis of  
623 the spread of hits from blastn interrogation of GenBank, but overall it seems that the reference  
624 library is currently the main limitation to study *Cocconeis* diversity by DNA metabarcoding. Due to  
625 the importance of these diatoms in marine attached communities, further efforts should be made to  
626 increasing their representation in the DNA reference library. A further and more worrying  
627 possibility is that some *Cocconeis* taxa may carry mutations in critical parts of one or both primer  
628 regions, but this too cannot be known without long reference sequences of the marine species. In  
629 contrast to *Cocconeis*, genera like *Pseudo-nitzschia*, *Haslea* and *Achnanthes* are well represented in  
630 the DNA reference database.

631 Finally, some discrepancies between methods can probably be attributed to variation among  
632 species in the *rbcL* copy number per cell, as noted previously by Vasselon et al. (2018), Kelly et al.

633 (2020) and Pérez-Burillo et al. (2020). This variation depends on the number of gene copies per  
634 chloroplast and the number of chloroplasts per cell. A correlation between the *rbcL* copy number  
635 and cell biovolume has been reported, leading to much higher relative abundances for high  
636 biovolume species, e.g., *Ulnaria ulna*, large *Pinnularia* or *Pleurosira laevis*, in metabarcoding  
637 outputs (Vasselon et al., 2018). This very likely explains the higher abundances obtained by the  
638 DNA method for *Achnanthes longipes* and *Pleurosigma*. These taxa are characterized by high  
639 biovolume and either high numbers of chloroplasts per cell (*A. longipes*) or highly complex, large  
640 chloroplasts (*Pleurosigma*).

#### 641 **Concluding remarks**

642 As mentioned earlier, diatoms can contribute well over 50% of primary benthic production in  
643 marine habitats where the only obvious photosynthetic organisms are seagrasses (Cox et al., 2020),  
644 while on apparently bare sediments lacking macrophytes, diatoms generally dominate, except in  
645 summer when cyanobacteria are often important (e.g., Scholz & Liebezeit, 2012b). Furthermore,  
646 individual diatom species, including species that coexist, can exhibit different responses to  
647 macronutrients (e.g., Underwood & Provot, 2000), different vertical migration patterns (Underwood  
648 et al., 2005), and different seasonality (e.g., Scholz & Liebezeit, 2012a). Hence, to understand  
649 marine benthic communities, it is important to identify and quantify species, and hence to have  
650 resources that facilitate consistent accurate identification.

651 The main aim of this paper was to use a small dataset to examine the advantages and disadvantages  
652 of metabarcoding and morphological approaches to study the benthic diatom communities of  
653 shallow coastal environments.-Our results show that both approaches are more difficult to  
654 implement than in freshwater environments and in both cases the cause is essentially the same:  
655 marine microphytobenthic communities have been greatly understudied, despite their ecological  
656 and economic importance. As a result, the traditional morphology-based taxonomy has yet to  
657 advance to the level achieved for freshwaters, while the lack of reference sequences limits the

658 resolution achievable with metabarcoding, though this did not prevent the molecular method from  
659 separating the samples according to the type of substratum. There are also special features of the  
660 marine benthos – such as the presence of a wider range of related microalgal groups – that offer  
661 extra opportunities for studying non-diatom diversity but also mean that the reference database  
662 needs to be more inclusive than in freshwaters for efficient identification of ASVs. Clearly, then,  
663 both approaches, morphological and metabarcoding, are in some senses incomplete for marine  
664 benthic diatom communities, but together they offer a strong foundation for ecological and  
665 biogeographical studies. We suggest that the way forward, for the moment, is to develop  
666 metabarcoding and morphological approaches in parallel and exploit their particular strengths and  
667 complementarity: for example, the far greater resolution and sensitivity of metabarcoding (and the  
668 albeit limited capacity to detect non-diatom components), combined with the insights into life-form,  
669 cell surface area: volume relationships and functional group membership that are inherent in the  
670 morphological approach and can never be fully realized with metabarcoding, even when the  
671 reference database is complete and allows all ASVs to be allocated to known species.

672

## 673 **Acknowledgments**

674 We acknowledge the Erasmus+ programme of the European Union which supported the traineeship  
675 of Greta Valoti (Università Politecnica delle Marche, Italy) in IRTA. J. Pérez-Burillo acknowledges  
676 IRTA and the Universitat Rovira i Virgili for his Martí Franqués PhD grant (2018PMF-PIPF-22).  
677 The Royal Botanic Garden Edinburgh is supported by the Scottish Government's Rural and  
678 Environment Science and Analytical Services Division. This article was facilitated by COST Action  
679 DNAqua-Net (CA15219), supported by the COST (European Cooperation in Science and  
680 Technology) program. We also acknowledge support from the CERCA Programme/ Generalitat de  
681 Catalunya. P Prado was contracted under the INIA-CCAA cooperative research program for  
682 postdoctoral incorporation from the Spanish National Institute for Agricultural and Food Research

683 and Technology (INIA). The authors would like to thank the Biodiversity Foundation from the  
684 Spanish Ministry for Ecological Transition for providing additional support for fieldwork sampling  
685 in the context of the Recupera Pinna project. Prof. Rafał J. Wróbel (West Pomeranian University of  
686 Technology) is acknowledged for his help with SEM examination of the diatomaceous samples. G.  
687 Valoti acknowledges Prof. Cecilia Totti (Università Politecnica delle Marche) for her support with  
688 respect to GV's IRTA visit. The authors would like to thank Vanessa Castan, IRTA technician, who  
689 collected the individuals of *Crassotrea gigas*. The authors state no conflicts of interest.

690

## 691 References

692 Adl, S.M., Bass, D., Lane, C.E., Lukeš, J., Schoch, C.L., Smirnov, A., Agatha, S., Berney, C.,  
693 Brown, M.W., Burki, F., Cárdenas, P., Čepička, I., Chistyakova, L., del Campo, J., Dunthorn,  
694 M., Edvardsen, B., Eglit, Y., Guillou, L., Hampl, V., Heiss, A.A., Hoppenrath, M., James,  
695 T.Y., Karnkowska, A., Karpov, S., Kim, E., Kolisko, M., Kudryavtsev, A., Lahr, D.J.G., Lara,  
696 E., Le Gall, L., Lynn, D.H., Mann, D.G., Massana, R., Mitchell, E.A.D., Morrow, C., Park,  
697 J.S., Pawlowski, J.W., Powell, M.J., Richter, D.J., Rueckert, S., Shadwick, L., Shimano, S.,  
698 Spiegel, F.W., Torruella, G., Youssef, N., Zlatogursky, V. & Zhang, Q. (2019). Revisions to  
699 the classification, nomenclature, and diversity of eukaryotes. *Journal of Eukaryotic*  
700 *Microbiology* 66: 4–119. <https://doi.org/10.1111/jeu.12691>

701 An, S.M., Choi, D.H. & Noh, J.H. 2020. High-throughput sequencing analysis reveals dynamic  
702 seasonal succession of diatom assemblages in a temperate tidal flat. *Estuar. Coast. Shelf Sci.*  
703 237. <https://doi.org/10.1016/j.ecss.2020.106686>

704 Andersen, R.A., Potter, D. & Bailey, J.C. 2002. *Pinguicoccus pyrenoidosus* gen. et sp. nov.  
705 (Pinguicophyceae), a new marine coccoid alga. *Phycol. Res.* 50: 57-65.

706 <https://dx.doi.org/10.1111/j.1440-1835.2002.tb00136.x>

- 707 Andrews, G.W. 1972. Some fallacies of quantitative diatom paleontology. *Nova Hedwigia, Beih.*  
708 39: 285–295.
- 709 Andriana, R., Engel, F.G., Gusmao, J.B., & Eriksson, B.K. 2021. Intertidal mussel reefs change the  
710 composition and size distribution of diatoms in the biofilm. *Mar. Biol.* 168: 24.  
711 <https://doi.org/10.1007/s00227-020-03819-2>
- 712 Bailet, B., Bouchez, A., Franc, A., Frigerio, J.-M., Keck, F., Karjalainen, S.-M., Rimet, F.,  
713 Schneider, S. & Kahlert, M. 2019. Molecular versus morphological data for benthic diatoms  
714 biomonitoring in Northern Europe freshwater and consequences for ecological status.  
715 *Metabarcoding and Metagenomics* 3: 21–35. <https://doi.org/10.3897/mbmg.3.34002>
- 716 Barille, L., Le Bris, A., Méléder, V., Launeau, P., Robin, M., Louvrou, I. & Ribeiro, L. 2017.  
717 Photosynthetic epibionts and endobionts of Pacific oyster shells from oyster reefs in rocky  
718 versus mudflat shores. *PLoS ONE* 12: e0185187.  
719 <https://doi.org/10.1371/journal.pone.0185187>
- 720 Belcher J.H. & Swale E.M.F. 1986. Notes on some small *Thalassiosira* species (Bacillariophyceae)  
721 from the plankton of the lower Thames and other British estuaries (identified by transmission  
722 electron microscopy). *Br. Phycol. J.* 21: 139–145.  
723 <https://doi.org/10.1080/00071618600650161>
- 724 Benito, X., Trobajo, R. & Ibáñez, C. 2015. Benthic diatoms in a Mediterranean delta: ecological  
725 indicators and a conductivity transfer function for paleoenvironmental studies. *J. Paleolimnol.*  
726 54: 171–188. <https://doi.org/10.1007/s10933-015-9845-3>
- 727 Benito, X., Trobajo, R., Cearreta, A. & Ibáñez, C. 2016. Benthic foraminifera as indicators of  
728 habitat in a Mediterranean delta: implications for ecological and palaeoenvironmental studies.  
729 *Estuar. Coast. Shelf Sci.* 180: 97–113. <https://doi.org/10.1016/j.ecss.2016.06.001>



730 Bombin, S., Wysor, B. & Lopez-Bautista, J.M. 2021. Assessment of littoral algal diversity from the  
731 northern Gulf of Mexico using environmental DNA metabarcoding. *J. Phycol.* 57: 269–278.  
732 <https://doi.org/10.1111/jpy.13087>

733 Cahoon, L.B. 1999. The role of benthic microalgae in neritic ecosystems. *Oceanogr. Mar. Biol.*  
734 *Ann. Rev.* 37: 47–86. <https://doi.org/10.1201/9781482298550-4>

735 Callahan, B.J., McMurdie, P.J., Rosen, M.J., Han, A.W., Johnson, A.J.A. & Holmes, S.P. 2016.  
736 DADA2: High resolution sample inference from Illumina amplicon data. *Nat. Methods.* 13:  
737 581–583. <https://doi.org/10.1038/nmeth.3869>

738 Camacho, C., Coulouris, G., Avagyan, V., Ma, N., Papadopoulos, J. & Bealer, K. 2009. BLAST  
739 plus: architecture and applications. *BMC Bioinform.* 10: 421. [https://doi.org/10.1186/1471-](https://doi.org/10.1186/1471-2105-10-421)  
740 [2105-10-421](https://doi.org/10.1186/1471-2105-10-421)

741 Camps-Castellà, J., Romero, J. & Prado P. 2020. Trophic plasticity in the sea urchin *Paracentrotus*  
742 *lividus*, as a function of resource availability and habitat features. *Mar Ecol Prog Ser.* 637:71-  
743 85. <https://doi.org/10.3354/meps13235>

744 Car, A., Witkowski, A., Dobosz, S., Jasprica, N., Ljubimir, S. & Zgłobicka, I. 2019. Epiphytic  
745 diatom assemblages on invasive *Caulerpa taxifolia* and autochthonous *Halimeda tuna* and  
746 *Padina* sp. seaweeds in the Adriatic Sea – summer/autumn aspect. *Oceanol Hidrobiol Stud.*  
747 48: 209–226. <https://doi.org/10.2478/ohs-2019-0019>

748 Carballeira, R., Trobajo, R., Leira, M., Benito, X., Sato, S. & Mann, D.G. 2017. A combined  
749 morphological and molecular approach to *Nitzschia varelae* sp. nov., with discussion of  
750 symmetry in Bacillariaceae. *Eur. J. Phycol.* 52: 342–359, DOI:  
751 <https://doi.org/10.1080/09670262.2017.1309575>

- 752 Chonova, T., Keck, F., Bouchez, A. & Rimet, F. 2020. A ready-to-use database for DADA2:  
753 Diat.barcode\_rbcL\_263bp\_DADA2 based on Diat.barcode v9. Portail Data INRAE, V2.  
754 <https://doi.org/10.15454/QBLSXP>
- 755 Cloern, J.E., Foster, S.Q. & Kleckner, A.E. 2013. Review: phytoplankton primary production in the  
756 world's estuarine-coastal ecosystems. *Biogeosci. Discuss.* 10:17725–17783.  
757 <https://doi.org/10.5194/bg-11-2477-2014>
- 758 Cox, T.E., Cebrian, J., Tabor, M., West, L. & Krause, J.W. 2020. Do diatoms dominate benthic  
759 production in shallow systems? A case study from a mixed seagrass bed. *Limnol Oceanogr.* 5:  
760 425-434. <https://doi.org/10.1002/lol2.10167>
- 761 Costanza, R., de Groot, R., Sutton, P., van der Ploeg, S., Anderson, S., Kubiszewski, I., Farber, S. &  
762 Turner, R. 2014. Changes in the global value of ecosystem services. *Global Environ. Change*  
763 26:152–158. <https://doi.org/10.1016/j.gloenvcha.2014.04.002>
- 764 D'Alelio, D., Cante, M.T., Russo, G.F., Totti, C. & De Stefano, M. 2011. Epizoic diatoms on  
765 gastropod shells: when substrate complexity selects for microcommunity complexity. *In*  
766 Dubinsky, Z. & Seckbach, J. [eds.] *All Flesh Is Grass. Plant-animal interrelationships.*  
767 Springer, Netherlands, pp. 349–364.
- 768 Deiner, K., Bik, H.M., Mächler, E., Seymour, M., Lacoursière-Roussel, A., Altermatt, F., Creer, S.,  
769 Bista, I., Lodge, D.M., Vere, N., Pfrender, M.E. & Bernatchez, L. 2017. Environmental DNA  
770 metabarcoding: Transforming how we survey animal and plant communities. *Mol. Ecol.* 26:  
771 5872–5895. <https://doi.org/10.1111/mec.14350>
- 772 De Luca, D., Piredda, R., Sarno, D. & Kooistra, W.H.C.F. 2021. Resolving cryptic species  
773 complexes in marine protists: phylogenetic haplotype networks meet global DNA  
774 metabarcoding datasets. *ISME J.* <https://doi.org/10.1038/s41396-021-00895-0>

775 De Stefano, M., Romero, O.E. & Totti, C. 2008. A comparative study of *Cocconeis scutellum*  
776 Ehrenberg and its varieties (Bacillariophyta). *Bot. Mar.* 51: 506–536.  
777 <https://doi.org/10.1515/BOT.2008.058>

778 Edgar, R.C. 2004. MUSCLE: multiple sequence alignment with high accuracy and high throughput.  
779 *Nucl. Acids Res.* 32: 1792–1797. <https://doi.org/10.1093/nar/gkh340>

780 Edler, D., Klein, J., Antonelli, A. & Silvestro, D. 2021. raxmlGUI 2.0: A graphical interface and  
781 toolkit for phylogenetic analyses using RAxML. *Methods Ecol. Evol.* 12: 373– 377.  
782 <https://doi.org/10.1111/2041-210X.13512>

783 Facca, C.A. & Sfriso, A. 2007. Epipelagic diatom spatial and temporal distribution and relationship  
784 with the main environmental parameters in coastal waters. *Estuar. Coast. Shelf Sci.* 75: 35–  
785 49. <https://doi.org/10.1016/j.ecss.2007.03.033>.

786 Goma, F., Utter, D.R., Powers, C., Beaudoin, D.J., Edgcomb, V.P., Filipsson, H.L., Hansel, C.M.,  
787 Wankel, S.D., Zhang, Y. & Bernhard, J.M. 2021. Multiple integrated metabolic strategies  
788 allow foraminiferan protists to thrive in anoxic marine sediments. *Sci. Adv.* 7: eabf1586.  
789 <https://doi.org/10.1126/sciadv.abf1586>

790 Gardner, C & Crawford, R.M. 1992. A description of the diatom *Papiliocellulus simplex* sp. nov.  
791 (Cymatosiraceae, Bacillariophyta) using light and electron microscopy. *Phycologia.* 31: 246-  
792 252. <https://doi.org/10.2216/i0031-8884-31-3-4-246.1>

793 Graf, L., Yang, E.C., Han, K.Y., Küpper, F.C., Benes, K.M., Oyadomari, J.K., Herbert, R.J.H.,  
794 Verbruggen, H., Wetherbee, R., Andersen, R.A. & Yoon, H.S. 2020. Multigene phylogeny,  
795 morphological observation and re-examination of the literature lead to the description of the  
796 Phaeosacciophyceae classis nova and four new species of the Heterokontophyta SI clade.  
797 *Protist* 171: 125781. <https://doi.org/10.1016/j.protis.2020.125781>

798 Grant, D.M., Brodnicke, O.B., Evankow, A.M., Ferreira, A.O., Fontes, J.T., Hansen, A.K.,  
799 Jensen, M.R., Kalaycı, T.E., Leeper, A., Patil, S.K., Prati, S., Reunamo, A., Roberts, A.J.,  
800 Shigdel, R., Tyukosova, V., Bendiksby, M., Blaaid, R., Costa, F.O., Hollingsworth, P.M.,  
801 Stur, E. & Ekrem, T. 2021. The future of DNA barcoding: reflections from early career  
802 researchers. *Diversity* 2021, 13: 313. <https://doi.org/10.3390/d13070313>

803 Guiry, G.M. 2021a. *Thalassiosira profunda*. In *AlgaeBase* (Ed. by M.D Guiry & G.M. Guiry).  
804 World-wide electronic publication, National University of Ireland, Galway.  
805 <http://www.algaebase.org>; searched on 16 July 2021.

806 Inoue, T. & Taniguchi, A. 1999. Seasonal distribution of vegetative cells and resting spores of the  
807 arcto-boreal diatom *Thalassiosira nordenskioeldii* Cleve in Onagawa Bay, northeastern Japan.  
808 In Mayama, I. & Koizumi, I. [eds.] *Proceedings of the 14th International Diatom Symposium*.  
809 Tokyo. pp. 263–276.

810 Jauffrais, T., LeKieffre, C., Schweizer, M., Geslin, E., Metzger, E., Bernhard, J.M., Jesus, B.,  
811 Filipsson, H.L., Mare, O. & Meiborn, A. 2019. Kleptoplastidic benthic foraminifera from  
812 aphotic habitats: insights into assimilation of inorganic C, N and S studied with sub-cellular  
813 resolution. *Env. Microbiol.* 21: 125–141. <https://doi.org/10.1111/1462-2920.14433>

814 Jeunen, G.-J., Knapp, M., Spencer, H.G., Lamare, M.D., Taylor, H.R. Stat, M., Bunce, M. &  
815 Gemmell, N.J. 2018. Environmental DNA (eDNA) metabarcoding reveals strong  
816 discrimination among diverse marine habitats connected by water movement. *Mol. Ecol.*  
817 *Resour.* 19: 426–438. <https://doi.org/10.1111/1755-0998.12982>

818 Kanjer, L., Mucko, M., Car, A. & Bosak, S. 2019. Epiphytic diatoms on *Posidonia oceanica* (L.)  
819 Delile leaves from eastern Adriatic Sea. *Nat. Croat.* 28: 1–20.  
820 <https://doi.org/10.20302/NC.2019.28.1>

821 Kelly, M.G., Juggins, S., Mann, D.G., Sato, S., Glover, R., Boonham, N., Sapp, M., Lewis, E.,  
822 Hany, U., Kille, P., Jones, T. & Walsh, K. 2020. Development of a novel metric for  
823 evaluating diatom assemblages in rivers using DNA metabarcoding. *Ecol. Indic.* 118: 106725.  
824 <https://doi.org/10.1016/j.ecolind.2020.106725>

825 Kermarrec, L., Franc, A., Rimet, F., Chaumeil, P., Frigerio, J.M., Humbert, J.F. & Bouchez, A.  
826 2014. A next-generation sequencing approach to river biomonitoring using benthic diatoms.  
827 *Freshw. Sci.* 33: 349–363. <https://doi.org/10.1086/675079>.

828 Krawczyk, D.W., Witkowski, A., Wroniecki, M., Waniek, J., Kurzydłowski, K.J. & Płociński, T.  
829 2012. Reinterpretation of two diatom species from the West Greenland margin —  
830 *Thalassiosira kushirensis* and *Thalassiosira antarctica* var. *borealis* – hydrological  
831 consequences. *Mar. Micropaleontol.* 88–89: 1–14.  
832 <https://doi.org/10.1016/j.marmicro.2012.02.004>.

833 Kumar, S., Stecher, G., Li, M., Knyaz, C. & Tamura, K. 2018. MEGA X: Molecular Evolutionary  
834 Genetics Analysis across computing platforms. *Mol. Biol. Evol.* 35: 1547–1549.  
835 <https://doi.org/10.1093/molbev/msy096>

836 Kuwata, A. & Takahashi, M. 1999. Survival and recovery of resting spores and resting cells of the  
837 marine planktonic diatom *Chaetoceros pseudocurvisetus* under fluctuating nitrate condition.  
838 *Mar. Biol.* 134: 471–478. <https://doi.org/10.1007/s002270050563>

839 Lee, J.J. 2011. Diatoms as endosymbionts. In Seckbach, J & Kociolek, P. [eds.] *The diatom world.*  
840 *Cellular Origin, Life in Extreme Habitats and Astrobiology.* Springer, Dordrecht. pp. 439 – 464.  
841 [https://doi.org/10.1007/978-94-007-1327-7\\_20](https://doi.org/10.1007/978-94-007-1327-7_20)

842 Letunic, I. & Bork, P. 2021. Interactive Tree Of Life (iTOL) v5: an online tool for phylogenetic tree  
843 display and annotation. *Nucl. Acids Res.* 49: W293–W296,  
844 <https://doi.org/10.1093/nar/gkab301>

- 845 Lewitus, A.J., Brock, L.M., Burke, M.K., DeMattio, K.A. & Wilde, S.B. 2008. Lagoonal  
846 stormwater detention ponds as promoters of harmful algal blooms and eutrophication along  
847 the South Carolina coast. *Harmful Algae*. 8: 60–65. <https://doi.org/10.1016/j.hal.2008.08.012>
- 848 Li, Ch-L., Witkowski, A., Ashworth, M.P., Dąbek, P., Sato, S., Zgłobicka, I., Witak, M., Khim, J.S.  
849 & Kwon, C.J. 2018. The morphology and molecular phylogenetics of some marine diatom  
850 taxa within the Fragilariaceae, including twenty undescribed species and their relationship to  
851 *Nanofrustulum*, *Opephora* and *Pseudostaurosira*. *Phytotaxa*. 355: 1–104.  
852 <https://doi.org/10.11646/phytotaxa.355.1.1>
- 853 Li, Y., Zhao, Q. & Lü, S. 2013. The genus *Thalassiosira* off the Guangdong coast, South China  
854 Sea. *Bot. Mar.* 56: 83-110. <https://doi.org/10.1515/bot-2011-0045>
- 855 Llebot, C., Solé, J., Delgado, M., Fernández-Tejedor, M., Campa, J. & Estrada, M. 2011.  
856 Hydrographical forcing and phytoplankton variability in two semi-enclosed estuarine bays. *J.*  
857 *Mar. Syst.* 86: 69–86. <https://doi.org/10.1016/j.jmarsys.2011.01.004>
- 858 Lobban, C.S., Schefter, M., Jordan, R.W., Arai, Y., Sasaki, A., Theriot, E.C., Ashworth, M., Ruck,  
859 E. & Chiara, P. 2012. Coral-reef diatoms (Bacillariophyta) from Guam: New records and  
860 preliminary checklist, with emphasis on epiphytic species from farmer-fish territories.  
861 *Micronesica*. 43: 237–479.
- 862 Mabrouk, L., Ben Brahim, M., Hamza, A., Mahfoudhi, M. & Bradai, M.N. 2014. A comparison of  
863 abundance and diversity of epiphytic microalgal assemblages on the leaves of the seagrasses  
864 *Posidonia oceanica* (L.) and *Cymodocea nodosa* (Ucria) Asch in Eastern Tunisia. *J. Mar. Biol.*  
865 2014: 1–10. <https://doi.org/10.1155/2014/275305>
- 866 MacIntyre, H.L., Geider, R.J. & Miller, D.C. 1996. Microphytobenthos: the ecological role of the secret  
867 garden of unvegetated, shallow-water marine habitats. I. Distribution, abundance and primary  
868 production. *Estuaries* 12:186–201. <https://doi.org/10.2307/1352224>

869 Malviya, S., Scalco, E., Audic, S., Vincent, F., Veluchamy, A., Poulain, J., Wincker, J., Ludicone,  
870 D., De Vargas, C., Bittner, L., Zingone, A. & Bowler, C. 2016. Insights into global diatom  
871 distribution and diversity in the world's ocean. *Proc. Natl. Acad. Sci.* 113:1516–1525.  
872 <https://doi.org/10.1073/pnas.1509523113>

873 Martin, M. 2011. Cutadapt removes adapter sequences from high-throughput sequencing reads.  
874 *EMBnet. J.* 17: 10–12. <https://doi.org/10.14806/ej.17.1.200>

875 Mann, D.G., Crawford, R.M. & Round, F.E. 2016. Bacillariophyta. In: Archibald, J.M., Simpson,  
876 A.G.B., Slamovits, C.H., Margulis, L., Melkonian, M., Chapman, D.J. & Corliss, J.O. [Eds.]  
877 *Handbook of the Protists*. Springer, Cham, New York, pp. 1–62. [https://doi.org/10.1007/978-](https://doi.org/10.1007/978-3-319-32669-6_29-1)  
878 [3-319-32669-6\\_29-1](https://doi.org/10.1007/978-3-319-32669-6_29-1).

879 McMurdie, P.J. & Holmes, S. 2013. phyloseq: An R package for reproducible interactive analysis  
880 and graphics of microbiome census data. *PLOS ONE* 8: e61217.  
881 <https://doi.org/10.1371/journal.pone.0061217>

882 McQuoid, M.R. & Hobson, L.A. 1996. Diatom resting stages. *J. Phycol.* 32: 889–902.  
883 <https://doi.org/10.1111/j.0022-3646.1996.00889.x>

884 Medlin, L.K. & Juggins, S. 2018. Multivariate analyses document host specificity, differences in  
885 the diatom metaphyton vs. epiphyton, and seasonality that structure the epiphytic diatom  
886 community. *Estuar. Coast. Shelf Sci.* 213: 314–330.  
887 <https://doi.org/10.1016/j.ecss.2018.06.011>

888 Mortágua, A., Vasselon, V., Oliveira, R., Elias, C., Chardon, C., Bouchez, A., Rimet, F., João Feio,  
889 M., & Almeida, S.F. 2019. Applicability of DNA metabarcoding approach in the  
890 bioassessment of Portuguese rivers using diatoms. *Ecol. Indic.* 106: 105470.  
891 <https://doi.org/10.1016/j.ecolind.2019.105470>.

892 Nunes, M., Lemley, D.A., Matcher, G.F. & Adams, J.B. 2021. The influence of estuary  
893 eutrophication on the benthic diatom community: a molecular approach. *Afr. J. Mar. Sci.* 43:  
894 171–186. <https://doi.org/10.2989/1814232X.2021.1897039>

895 Oksanen, J., Guillaume Blanchet, F., Friendly, M., Kindt, R., Legendre, P., McGlinn, D., Minchin,  
896 P.R., O'Hara, B., Simpson, G.L., Solymos, P., Stevens, M.H.H., Szoecs, E. & Wagner, H.  
897 2020. Vegan: Community Ecology Package. R package, version 2.5-7. [https://CRAN.R-](https://CRAN.R-project.org/package=vegan)  
898 [project.org/package=vegan](https://CRAN.R-project.org/package=vegan)

899 Park, J.S., Jung, S.W., Lee, J.H., Yun, S.M. & Lee, J.H. 2016. Species diversity of the genus  
900 *Thalassiosira* (Thalassiosirales, Bacillariophyta) in South Korea and its biogeographical  
901 distribution in the world. *Phycologia* 55: 403–423. <https://doi.org/10.2216/15-66.1>

902 Passy, S.I. 2007. Diatom ecological guilds display distinct and predictable behavior along nutrient  
903 and disturbance gradients in running waters. *Aquat. Bot.* 86: 171–178.  
904 <https://doi.org/10.1016/j.aquabot.2006.09.018>

905 Percopo, I., Siano, R., Cerino, F., Sarno, D. & Zingone, A. 2011. Phytoplankton diversity during the  
906 spring bloom in the northwestern Mediterranean Sea. *Bot. Mar.* 54: 243–267.  
907 <https://doi.org/10.1515/bot.2011.033>

908 Pérez-Burillo, J., Trobajo, R., Vasselon, V., Rimet, F., Bouchez, A. & Mann, D.G. 2020. Evaluation  
909 and sensitivity analysis of diatom DNA metabarcoding for WFD bioassessment of  
910 Mediterranean rivers. *Sci. Total Environ.* 727: 138445.  
911 <https://doi.org/10.1016/j.scitotenv.2020.138445>

912 Pérez-Burillo, J., Trobajo, R., Leira, M., Keck, F., Rimet, F., Sigró, J. & Mann, D.G. 2021. DNA  
913 metabarcoding reveals differences in distribution patterns and ecological preferences among  
914 genetic variants within some key freshwater diatom species. *Sci. Total Environ.* 728: 149029.  
915 <https://doi.org/10.1016/j.scitotenv.2021.149029>



- 916 Pillet, L., de Vargas, C. & Pawlowski, J. 2011. Molecular identification of sequestered diatom  
917 chloroplasts and kleptoplastidy in foraminifera. *Protist* 162: 394–404.  
918 <https://doi.org/10.1016/j.protis.2010.10.001>
- 919 Piredda, R., Claverie, J.-M., Decelle, J., De Vargas, C., Dunthorn, M., Edvardsen, B., Eikrem, W.,  
920 Forster, D., Kooistra, W.H.C.F., Logares, R., Massana, R., Montresor, M., Not, F., Ogata, H.,  
921 Pawlowski, J., Romac, S., Sarno, D., Stoeck, T. & Zingone, A. 2018. Diatom diversity  
922 through HTS-metabarcoding in coastal European seas. *Sci. Rep.* 8: 18059.  
923 <https://doi.org/10.1038/s41598-018-36345-9>
- 924 Plante, C.J., Hill-Spanik, K., Cook, M. & Graham, C. 2021a. Environmental and spatial influences  
925 on biogeography and community structure of saltmarsh benthic diatoms. *Estuaries Coasts*.  
926 44: 147–161. <https://doi.org/10.1007/s12237-020-00779-0>
- 927 Plante, C.J., Hill-Spanik, K. & Lowry, J. 2021b. Controls on diatom biogeography on South  
928 Carolina (USA) barrier island beaches. *Mar. Ecol. Progr. Ser.* 661: 17–33. DOI:  
929 <https://doi.org/10.3354/meps13598>
- 930 Polifrone, M., Viera-Rodríguez, M.A., Pennesi, C., Conte, M.T., Del Pino, A.S., Stroobant, M. &  
931 De Stefano, M. 2020. Epiphytic diatoms on Gelidiales (Rhodophyta) from Gran Canaria  
932 (Spain). *Eur. J. Phycol.* 55: 404–411. <https://doi.org/10.1080/09670262.2020.1737967>
- 933 Prado, P., Caiola, N. & Ibañez, C. 2014. Habitat use by a large population of *Pinna nobilis* in  
934 shallow waters. *Sci. Mar.* 78: 555–565. <https://doi.org/10.3989/scimar.04087.03A>
- 935 Prado, P. 2018. Seagrass epiphytic assemblages are strong indicators of agricultural discharge but  
936 weak indicators of host features. *Estuar. Coast. Shelf Sci.* 204: 140–148.  
937 <https://doi.org/10.1016/j.ecss.2018.02.026>
- 938 Prado, P., Andree, K.B., Trigos, S., Carrasco, N., Caiola, N., García-March, J.R., Tena, J.,  
939 Fernández-Tejedor, M. & Carella, F. 2020. Breeding, planktonic and settlement factors shape

940 recruitment patterns of one of the last remaining major population of *Pinna nobilis* within  
941 Spanish waters. *Hydrobiologia*. 847: 771–786. <https://doi.org/10.1007/s10750-019-04137-5>

942 Prado, P., Grau, A., Catanese, G., Cabanes, P., Carella, F., Fernández-Tejedor, M., Andree, K.B.,  
943 Añón, T., Hernandis, S., Tena, J., García-March, J.R. 2021. *Pinna nobilis* in suboptimal  
944 environments are more tolerant to disease but more vulnerable to severe weather phenomena.  
945 *Mar. Environ. Res.* 163: 105220. <https://doi.org/10.1016/j.marenvres.2020.105220>

946 Ramón, M., Cano, J., Peña, J.B., & Campos, M.J. 2005. Current status and perspectives of mollusc  
947 (bivalves and gastropods) culture in the Spanish Mediterranean. *Bol. Inst. Esp. Oceanogr.* 21:  
948 361–373.

949 Rimet, F. & A. Bouchez. 2012. Life-forms, cell-sizes and ecological guilds of diatoms in European  
950 rivers. *Knowl. Manag. Aquat. Ecosyst.* 406: 1–14. doi:10.1051/kmae/2012018

951 Rimet, F., Vasselon, V., A.-Keszte, B. & Bouchez, A. 2018. Do we similarly assess diversity with  
952 microscopy and high-throughput sequencing? Case of microalgae in lakes. *Org. Divers. Evol.*  
953 18: 51–62. <https://doi.org/10.1007/s13127-018-0359-5>.

954 Rimet, F., Gusev, E., Kahlert, M., Kelly, M.G., Kulikovskiy, M., Maltsev, Y., Mann, D.G.,  
955 Pfannkuchen, M., Trobajo, R., Vasselon, V., Zimmermann, J. & Bouchez, A. 2019.  
956 Diat.barcode, an open-access curated barcode library for diatoms. *Sci.Rep.* 9: 1–12.  
957 <https://doi.org/10.1038/s41598-019-51500-6>.

958 Rivera, S.F., Vasselon, V., Ballorain, K., Carpentier, A., Wetzel, C.E., Ector, L., Bouchez, A. &  
959 Rimet, F. 2018. DNA metabarcoding and microscopic analyses of sea turtles biofilms:  
960 complementary to understand turtle behavior. *PLoS ONE*, 13(4): e0195770.  
961 <https://doi.org/10.1371/journal.pone.0195770>

962 Round, F.E. 1971. Benthic marine diatoms. *Oceanogr. Mar. Biol. Ann. Rev.* 9:83–139.

- 963 Round, F.E., Crawford, R.M. & Mann, D.G. 1990. *The diatoms. Biology and morphology of the*  
964 *genera*. Cambridge University Press, Cambridge.
- 965 Rovira, L., Trobajo, R. & Ibañez, C. 2009. Periphytic diatom community in a Mediterranean salt  
966 wedge estuary: the Ebro Estuary (NE Iberian Peninsula). *Acta Bot. Croat.* 68: 285–300.
- 967 Ryabushko, L.I. & Ryabushko, V.I. 2000. Communities of diatoms on the shells of mollusks of the  
968 genus *Mytilus* L. *Int. J. Algae.* 2: 15–22. <https://doi.org/10.1615/InterJAlgae.v2.i2.20>
- 969 Schmidt, C., Morard, R., Romero, O. & Kucera, M. 2018. Diverse Internal Symbiont Community in  
970 the Endosymbiotic Foraminifera *Pararotalia calcariformata*: Implications for Symbiont  
971 Shuffling Under Thermal Stress. *Front Microbiol.* 9: 2018.  
972 <https://doi.org/10.3389/fmicb.2018.02018>
- 973 Schmidt, M., Horn, S., Flieger, K., Ehlers, K., Wilhelm, C. & Schnetter, R. 2012. *Synchroma*  
974 *pusillum* sp. nov. and other new algal isolates with chloroplast complexes confirm the  
975 Synchronomphyceae (Ochrophyta) as a widely distributed group of amoeboid algae. *Protist.*  
976 163: 544–559. <https://doi.org/10.1016/j.protis.2011.11.009>
- 977 Scholz, B. & Liebezeit, G. 2012a. Microphytobenthic dynamics in a Wadden Sea intertidal flat –  
978 Part I: seasonal and spatial variation of diatom communities in relation to macronutrient  
979 supply. *Eur. J. Phycol.* 47: 105–119. <https://doi.org/10.1080/09670262.2012.663793>
- 980 Scholz, B. & Liebezeit, G. 2012b. Microphytobenthic dynamics in a Wadden Sea intertidal flat –  
981 Part II: seasonal and spatial variability of non-diatom community components in relation to  
982 abiotic parameters. *Eur. J. Phycol.* 47: 120–137.  
983 <https://doi.org/10.1080/09670262.2012.665251>
- 984 Stamatakis, A. 2014. Raxml version 8: a tool for phylogenetic analysis and post-analysis of large  
985 phylogenies. *Bioinformatics* 30:1312–1313. <https://doi.org/10.1093/bioinformatics/btu033>

- 986 Stoof-Leichsenring, K.R., Pestryakova, L.A., Epp, L.S. & Herzsuh, U. 2020. Phylogenetic  
987 diversity and environment form assembly rules for Arctic diatom genera—A study on recent  
988 and ancient sedimentary DNA. *J. Biogeogr.* 47: 1166–1179. <https://doi.org/10.1111/jbi.13786>
- 989 Sugie, K. & Kuma, K. 2008. Resting spore formation in the marine diatom *Thalassiosira*  
990 *nordenskioeldii* under iron- and nitrogen-limited conditions, *J. Plankton. Res.* 30: 1245–1255,  
991 <https://doi.org/10.1093/plankt/fbn080>
- 992 Sundbäck, K. & Granéli, W. 1988. Influence of microphytobenthos on the nutrient flux between  
993 sediment and water: A laboratory study. *Mar. Ecol. Prog. Ser.* 43: 63–69.  
994 <https://doi.org/10.3354/meps043063>
- 995 Sundbäck, K., Enoksson, V., Granéli, W. & Pettersson, K. 1991. Influence of sublittoral  
996 microphytobenthos on the oxygen and nutrient flux between sediment and water: A laboratory  
997 continuous-flow study. *Mar. Ecol. Prog. Ser.* 74: 263–279.  
998 <https://doi.org/10.3354/meps074263>
- 999 Takano, Y., Hansen, G., Fujita, D. & Horiguchi, T. 2007. Serial replacement of diatom  
1000 endosymbionts in two freshwater dinoflagellates, *Peridiniopsis* spp. (Peridinales,  
1001 Dinophyceae). *Phycologia* 47: 41–53. <https://doi.org/10.2216/07-36.1>
- 1002 Totti, C., Romagnoli, T., De Stefano, M., Di Camillo, C.G. & Bavestrello, G. 2011. The diversity of  
1003 epizoic diatoms: relationships between diatoms and marine invertebrates. In Dubinsky, Z. &  
1004 Seckbach, J. [eds.] *All Flesh Is Grass. Plant-Animal Interrelationships*. Springer,  
1005 Netherlands, pp. 327–343.
- 1006 Triska, F.J. & Oremland, R.S. 1981. Denitrification associated with periphyton communities. *Appl.*  
1007 *Environ. Microbiol.* 42: 745–748. <https://doi.org/10.1128/aem.42.4.745-748.1981>
- 1008 Trobajo, R. & Sullivan, M.J. 2010. Applied diatom studies in estuaries and shallow coastal  
1009 environments. In Smol, J.P. & Stoermer, E.F.[eds.] *The Diatoms: Applications for the*

1010 *Environmental and Earth Sciences*. Cambridge University Press, Cambridge, UK. pp 309–  
1011 323.

1012 Trobajo, R., Quintana, X.D. & Sabater, S. 2004. Factors affecting the periphytic diatom community  
1013 in Mediterranean coastal wetlands (Empordà wetlands, NE Spain). *Arch. Hydrobiol.* 160:  
1014 375–399. <https://doi.org/10.1127/0003-9136/2004/0160-0375>

1015 Underwood, G.J.C. & Provot, L. 2000. Determining the environmental preferences of four epipelagic  
1016 diatom taxa: growth across a range of salinities, nitrate and ammonium conditions. *Eur. J.*  
1017 *Phycol.* 35: 173–182. <https://doi.org/10.1080/09670260010001735761>

1018 Underwood, G.J.C., Perkins, R.G., Consalvey, M.C., Hanlon, A.R.M., Oxborough, K., Baker, N.R.  
1019 & Paterson, D.M. 2005. Patterns in microphytobenthic primary productivity: Species-specific  
1020 variation in migratory rhythms and photosynthetic efficiency in mixed-species biofilms.  
1021 *Limnol. Oceanogr.* 50: 755–767. <https://doi.org/10.4319/lo.2005.50.3.0755>.

1022 Vasselon, V., Rimet, F., Tapolczai, K. & Bouchez, A. 2017. Assessing ecological status with  
1023 diatoms DNA metabarcoding: scaling-up on aWFD monitoring network (Mayotte island,  
1024 France). *Ecol. Indic.* 82: 1–12. <https://doi.org/10.1016/j.ecolind.2017.06.024>

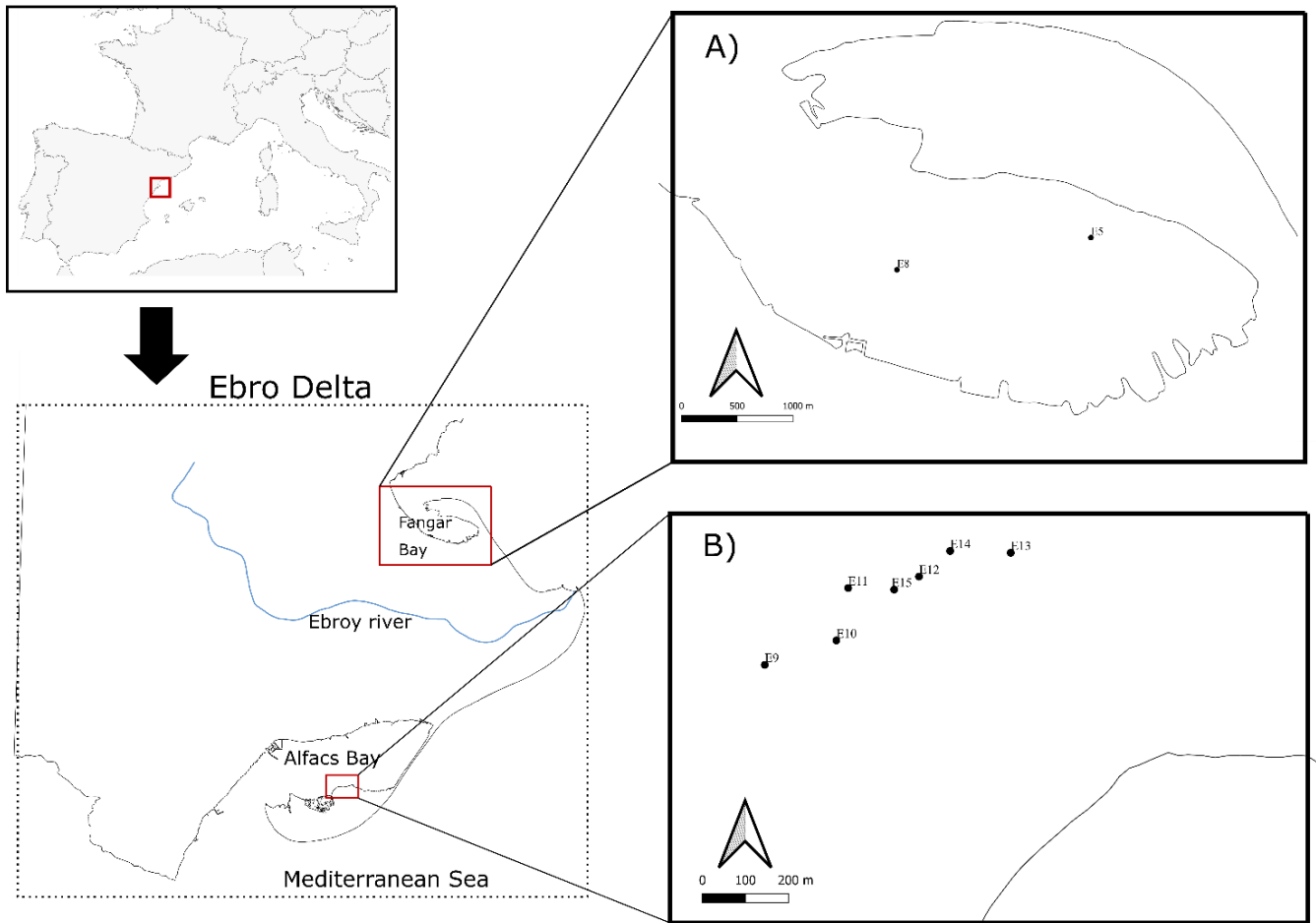
1025 Vasselon, V., Bouchez, A., Rimet, F., Jacquet, S., Trobajo, R., Corniquel, M., Tapolczai, K. &  
1026 Domaizon, I. 2018. Avoiding quantification bias in metabarcoding: application of a cell  
1027 biovolume correction factor in diatom molecular biomonitoring. *Methods Ecol. Evol.* 9:  
1028 1060–1069. <https://doi.org/10.1111/2041-210X.12960>

1029 Virta, L., Gammal, J., Järnström, M., Bernard, G., Soininen, J., Norkko, J. & Norkko, A. 2019. The  
1030 diversity of benthic diatoms affects ecosystem productivity in heterogeneous coastal  
1031 environments. *Ecology* 100: e02765. <https://doi.org/10.1002/ecy.2765>

- 1032 Wang, Q., Garrity, G.M., Tiedje, J.M. & Cole, J.R. 2007. Naïve Bayesian classifier for rapid  
1033 assignment of rRNA sequences into the new bacterial taxonomy. *Appl. Environ. Microbiol.*  
1034 73: 5261–5267. <https://doi.org/10.1128/AEM.00062-07>
- 1035 Wetherbee, R., Bringloe, T.T., Costa, J.F., van de Meene, A., Andersen, R.A. & Verbruggen, H.  
1036 2021. New pelagophytes show a novel mode of algal colony development and reveal a  
1037 perforated theca that may define the class. *J. Phycol.* 57: 396–411.  
1038 <https://doi.org/10.1111/jpy.13074>
- 1039 Witak, M., Pędziński, J., Olwa, S. & Hetko, D. (2020). Biodiversity of benthic diatom flora in the  
1040 coastal zone of Puck Bay (southern Baltic Sea): a case study of the Hel Peninsula. *Oceanol.*  
1041 *Hydrobiol. Studies* 49: 304–318. <https://doi.org/10.1515/ohs-2020-0027>
- 1042 Yamada, N., Bolton, J.J., Trobajo, R., Mann, D.G., Dąbek, P., Witkowski, A., Onuma, R.,  
1043 Horiguchi, T. & Kroth, P.G. 2019. Discovery of a kleptoplastic ‘dinotom’ dinoflagellate and  
1044 the unique nuclear dynamics of converting kleptoplastids to permanent plastids. *Sci. Rep.* 9:  
1045 10474. <https://doi.org/10.1038/s41598-019-46852-y>
- 1046 Yamada, N., Sakai, H., Onuma, R., Kroth, P.G. & Horiguchi, T. 2020. Five non-motile dinotom  
1047 dinoflagellates of the genus *Dinothrix*. *Front. Plant Sci.* 11: 1764.
- 1048 You, X., Luo, Z., Su, Y., Gu, L. & Gu, H. 2015. *Peridiniopsis jiulongensis*, a new freshwater  
1049 dinoflagellate with a diatom endosymbiont from China. *Nova Hedwigia* 101: 313–326.  
1050 [https://doi.org/10.1127/nova\\_hedwigia/2015/0272](https://doi.org/10.1127/nova_hedwigia/2015/0272)
- 1051 Zgrundo, A., Lemke, P., Pniewski, F., Cox, E.J., Latala, A. 2013. Morphological and molecular  
1052 phylogenetic studies on *Fistulifera saprophila*. *Diat. Res.* 28: 431–443. [https://](https://doi.org/10.1080/0269249X.2013.833136)  
1053 [doi.org/10.1080/0269249X.2013.833136](https://doi.org/10.1080/0269249X.2013.833136).

1054 Zimmermann, J., Glöckner, G., Jahn, R., Enke, N. & Gemeinholzer, B. 2015. Metabarcoding vs.  
1055 morphological identification to assess diatom diversity in environmental studies. *Mol. Ecol.*  
1056 *Resour.* 15: 526–542. <https://doi.org/10.1111/1755-0998.12336>.

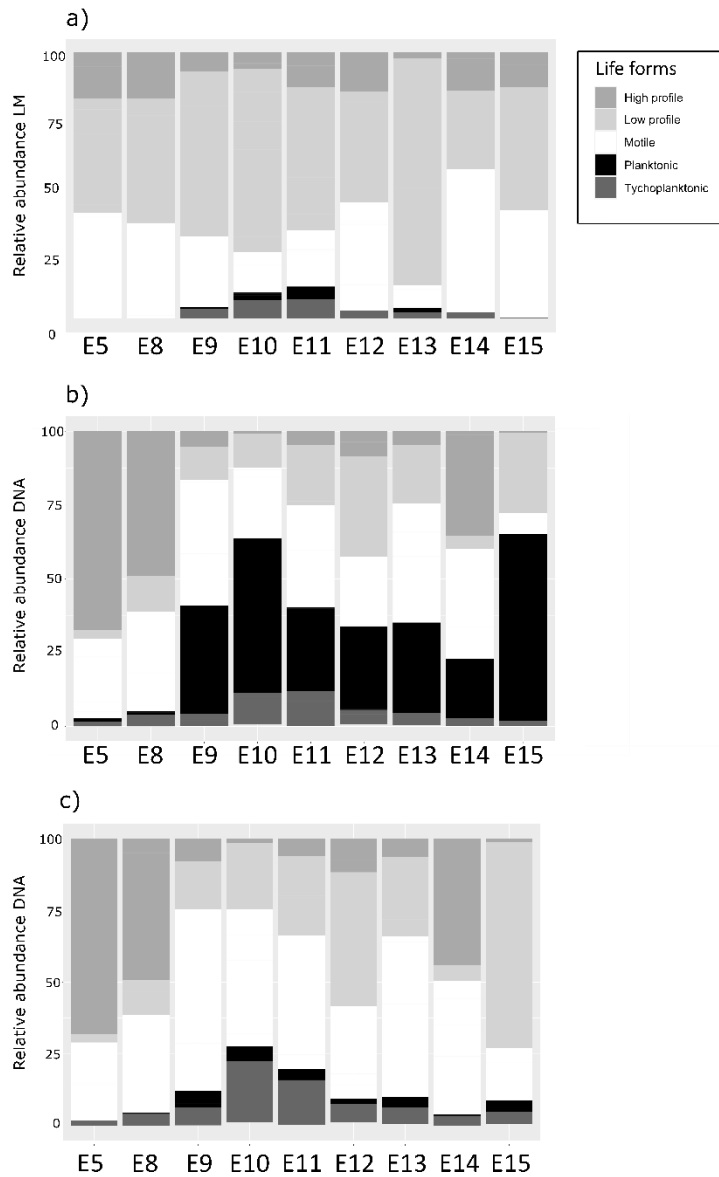
1057



1059

1060 Fig 1. Location of Ebro Delta (NE of Spain) and samples sites of Fangar (A) and Alfacs (B) bays. 2 biofilms  
 1061 samples (E5 and E8) were taken from the surface of *Crassostrea gigas* individuals located in the Fangar Bay  
 1062 (A). 7 biofilms samples were taken from the surface of *Pinna nobilis* (E9, E11 and E12), *Cymodocea nodosa*  
 1063 (E14) and *Caulerpa prolifera* (E15) individuals located in the Alfacs Bay (B). The eediment samples (E10  
 1064 and E13) were taken from the sediment adjacent to specimens of *P.nobilis* located in the Alfacs Bay (B).





1065

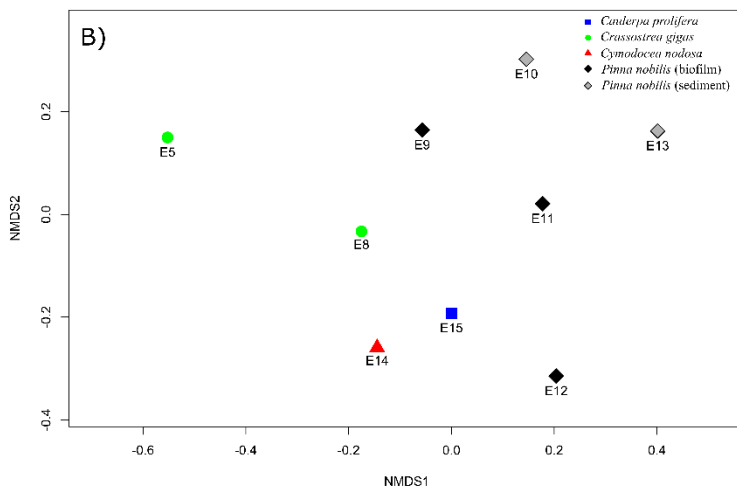
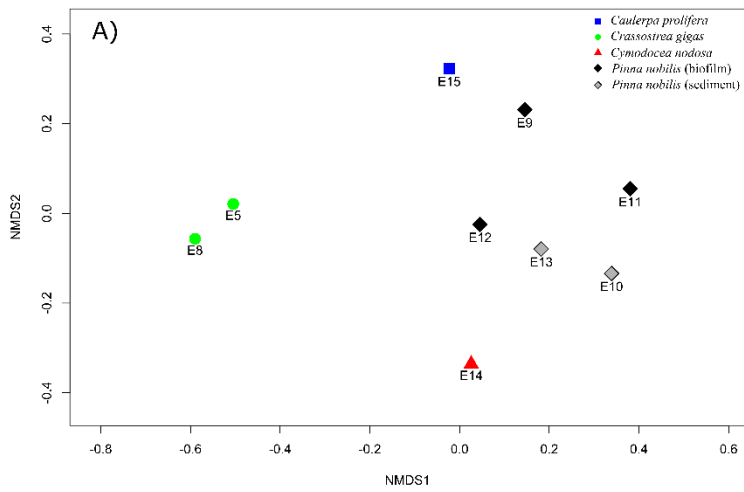
1066

1067

1068

1069

Fig 2. Relative abundance comparison of diatom growth forms between LM (a), DNA metabarcoding inventories (b) and DNA metabarcoding without considering the planktonic species *Thalassiosira profunda* (c).

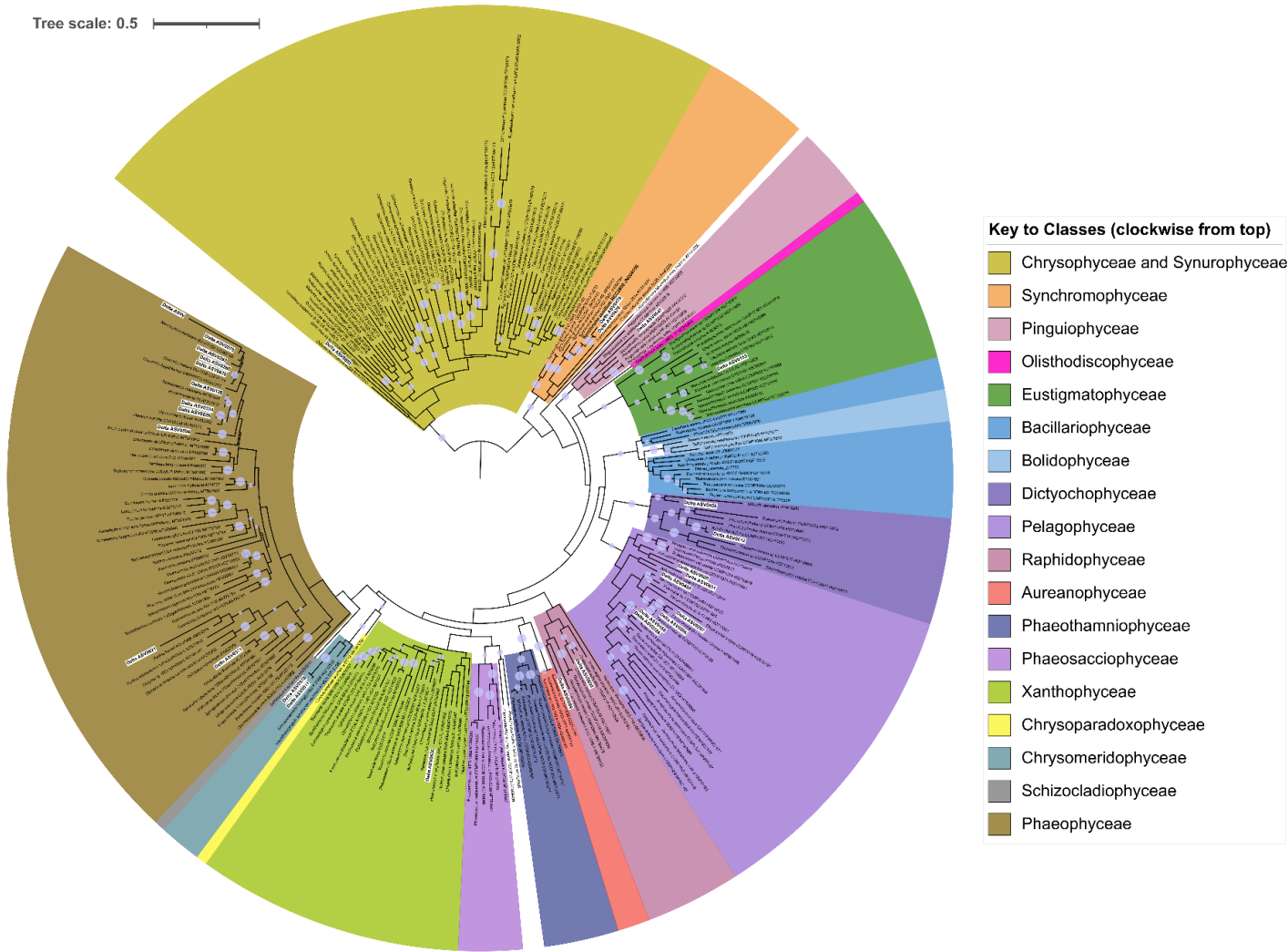


1070

1071 Figure 3. Non-metric multidimensional scaling of the Bray-Curtis dissimilarity calculated on diatom ASVs  
 1072 relative abundance (A; stress=0.09) and relative abundance of diatom taxa identified by LM (B; stress=0.13).

1073

1074



1075

1076 Fig 4. Maximum likelihood phylogenetic tree based on non-diatom ASVs related to different heterokont  
 1077 classes. *RbcL* representative sequences included in the tree were extracted from Graf et al. (2020),  
 1078 Watherbee et al. (2021) and GenBank database. The tree was built using using raxmlGUI on an alignment  
 1079 partitioned by codon position and setting the GRT-Gamma model with 1000 replicates for the bootstrap  
 1080 analyses. The tree was drawn using iTOL. Bootstrap support values from 70 to 100 are represented. ASVs  
 1081 from *rbcL* metabarcoding are highlighted by white boxes.

1082

1083 Tables

1084 Table 1: Physico-chemical measurements registered in the different sampling sites at the time and date of  
 1085 sampling. Note that there are samples (E9 & E10; E12-E15) with the same physico-chemical data; this is  
 1086 because these samples were collected on the same date from the same small area, being separated from each  
 1087 other by distances in the order of 10s of meters.

1088

Sample	Sampling date	Sampling time	Water temperature (°C)	Salinity (g/L)	pH	Dissolved oxygen (mg/L)	% Dissolved oxygen (mg/L)
E5 - <i>Crassostrea gigas</i>	03/03/2020	12:35	11	35.87	7.95	7.49	85.1
E8 - <i>Crassostrea gigas</i>	10/03/2020	13:00	12.3	36.99	8.05	6.97	82.2
E9 - <i>Pinna nobilis</i> biofilm	12/03/2020	12:15	14.9	36.5	8.11	7.79	96.7
E10 - <i>Pinna nobilis</i> sediment							
E11 - <i>Pinna nobilis</i> biofilm	12/03/2020	14:30	16.6	37.27	8.24	8.65	111.6
E12 - <i>Pinna nobilis</i> biofilm	12/03/2020	15:50	15.4	36.24	8.14	7.72	97.6
E13 - <i>Pinna nobilis</i> sediment							
E14 - <i>Cymodocea nodosa</i>							
E15 - <i>Caulerpa prolifera</i>							

1089

1090 Table 2. Comparison of taxa richness and Shannon diversity index values obtained for the LM and DNA  
1091 metabarcoding methods.

1092

Sample	Microscopy		DNA metabarcoding	
	Taxa richness	Shannon index	Taxa richness	Shannon index
E5 - <i>Crassostrea gigas</i>	69	3.50	37	2.15
E8 - <i>Crassostrea gigas</i>	48	2.90	52	2.92
E9 - <i>Pinna nobilis</i> biofilm	44	2.81	37	2.43
E10 - <i>Pinna nobilis</i> sediment	75	3.73	47	2.23
E11 - <i>Pinna nobilis</i> biofilm	71	3.74	62	3.04
E12 - <i>Pinna nobilis</i> biofilm	67	3.46	55	3.04
E13 - <i>Pinna nobilis</i> sediment	72	3.50	57	2.88
E14 - <i>Cymodocea nodosa</i>	40	2.61	35	2.21
E15 - <i>Caulerpa prolifera</i>	44	3.34	25	1.59

1093

1094

1095 Table 3. SIMPER analyses showing taxa contribution to the total dissimilarities between DNA  
 1096 metabarcoding and LM methods. Only the first thirty taxa with the greatest contribution to dissimilarities are  
 1097 shown. It is also indicated the taxa for which there are or not representative sequences in the reference library  
 1098 Diat.barcode v9.

1099

Taxon	Relative abundance DNA metabarcoding	Relative abundance LM	Contribution to dissimilarities (%)	Cumulative Contribution to dissimilarities (%)	Availability of a representative sequence in Diat.barcode v9
<i>Thalassiosira profunda</i>	27.36	0	14.37	14.37	yes
<i>Navicula sp.4</i>	0	9.3	4.88	19.25	no
<i>Amphora helenensis</i>	1.74	9.08	4.27	23.52	yes
<i>Achnanthes longipes</i>	7.64	0.45	4.15	27.67	yes
<i>Berkeleya fennica</i>	7.17	2.02	3.51	31.18	yes
<i>Nanofrustulum shiloi</i>	5.17	2.61	2.97	34.15	yes
<i>Navicula sp.</i>	4.47	0	2.35	36.50	yes
<i>Amphora cf.helenensis</i>	0	4.17	2.19	38.69	yes
<i>Nitzschia spathulata</i>	3.57	0	1.87	40.56	no
<i>Cocconeis scutellum v. posidoniae</i>	0	3.47	1.82	42.38	no
<i>Navicula normaloides</i>	0	2.89	1.52	43.90	yes
<i>Haslea howeana</i>	2.79	0	1.47	45.37	no
<i>Cyclotella choctawhatcheeana</i>	0.11	2.77	1.43	46.80	yes
<i>Navicula normalis</i>	0	2.69	1.41	48.21	no
<i>Cocconeis scutellum</i>	0	2.56	1.35	49.56	no
<i>Cyclotella sp.</i>	2.15	0	1.13	50.68	yes
<i>Seminavis robusta</i>	1.57	0.92	1.11	51.79	yes
<i>Nitzschia sp.</i>	2.02	0	1.06	52.86	yes
<i>Pleurosigma sp.</i>	1.94	0	1.02	53.88	yes
<i>Halamphora sp.2</i>	0	1.81	0.95	54.83	yes
<i>Navicula perminuta</i>	1.75	0.53	0.92	55.75	no
<i>Serratifera sp.3</i>	0	1.71	0.90	56.65	no
<i>Plagiogramma minus</i>	0	1.71	0.90	57.55	no
<i>Seminavis cf. robusta</i>	1.69	0	0.89	58.43	yes
<i>Navicula subagnita</i>	0	1.68	0.88	59.31	no
<i>Pteroncola marina</i>	0	1.43	0.75	60.06	yes
<i>Craspedostauros constricta</i>	1.42	0	0.74	60.81	yes
<i>Psammodictyon sp.</i>	1.39	0	0.73	61.54	no
<i>Mastogloia crucicula</i>	0	1.36	0.72	62.26	yes
<i>Halamphora sp.</i>	1.36	0	0.71	62.97	no

1100

1101